Biomolecular Feedback Systems

Domitilla Del Vecchio
MIT

Richard M. Murray
Caltech

DRAFT v0.4b, January 23, 2011

Chapter 3
Analysis of Dynamic Behavior

In this chapter, we describe some of the tools from dynamical systems and feed-back control theory that will be used in the rest of the text to analyze and design biological circuits, building on tools already described in AM08. We focus here on deterministic models and the associated analyses; stochastic methods are given in Chapter 4.

Prerequisites. Readers should have a understanding of the tools for analyzing sta-bility of solutions to ordinary differential equations, at the level of Chapter 4 of AM08. We will also make use of linearized input/output models in state space, based on the techniques described in Chapter 5 of AM08, and sensitivity function methods, described in Chapters 11 and 12 of AM08 and building on the frequency domain techniques described in Chapters 8–10.

3.1   Input/Output Modeling [AM08]

In the previous chapter we constructed a variety of models to capture the dynamic behavior of a biomolecular subsystem. In this chapter we expand on that treatment by including external inputs and measured outputs as a part of the description of the system (or a portion of the system).

The Heritage of Electrical Engineering

The approach to modeling that we take builds on the view of models that emerged from electrical engineering, where the design of electronic amplifiers led to a focus on input/output behavior. A system was considered a device that transforms inputs to outputs, as illustrated in Figure 3.1. Conceptually an input/output model can be viewed as a giant table of inputs and outputs. Given an input signal $u(t)$ over some interval of time, the model should produce the resulting output $y(t)$.

The input/output framework is used in many engineering disciplines since it allows us to decompose a system into individual components connected through their inputs and outputs. Thus, we can take a complicated system such as a radio or a television and break it down into manageable pieces such as the receiver, demod-ulator, amplifier and speakers. Each of these pieces has a set of inputs and outputs and, through proper design, these components can be interconnected to form the entire system.
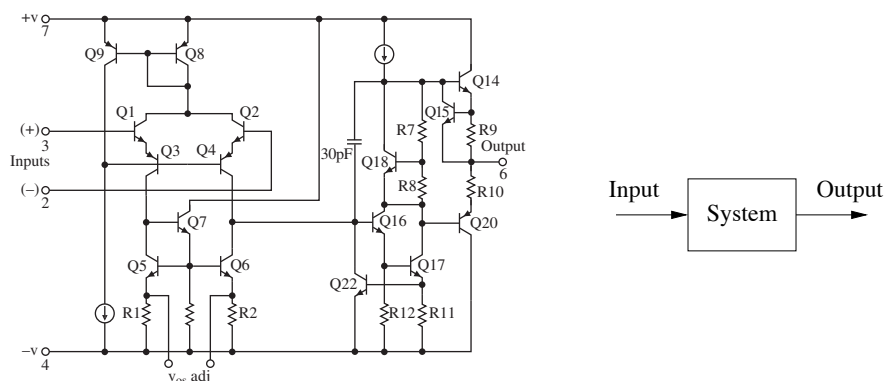
Figure 3.1: Illustration of the input/output view of a dynamical system. The figure on the left shows a detailed circuit diagram for an electronic amplifier; the one on the right is its representation as a block diagram.

The input/output view is particularly useful for the special class of *linear time-invariant systems*. This term will be defined more carefully below, but roughly speaking a system is linear if the superposition (addition) of two inputs yields an output that is the sum of the outputs that would correspond to individual inputs being applied separately. A system is time-invariant if the output response for a given input does not depend on when that input is applied. While most biomolecular systems are neither linear nor time-invariant, they can often be approximated by such models, often by looking at perturbations of the system from its nominal behavior, in a fixed context.

One of the reasons that linear time-invariant systems are so prevalent in modeling of input/output systems is that a large number of tools have been developed to analyze them. One such tool is the *step response*, which describes the relationship between an input that changes from zero to a constant value abruptly (a step input) and the corresponding output. The step response is very useful in characterizing the performance of a dynamical system, and it is often used to specify the desired dynamics. A sample step response is shown in Figure 3.2a.

Another way to describe a linear time-invariant system is to represent it by its response to sinusoidal input signals. This is called the *frequency response*, and a rich, powerful theory with many concepts and strong, useful results has emerged. The results are based on the theory of complex variables and Laplace transforms. The basic idea behind frequency response is that we can completely characterize the behavior of a system by its steady-state response to sinusoidal inputs. Roughly speaking, this is done by decomposing any arbitrary signal into a linear combination of sinusoids (e.g., by using the Fourier transform) and then using linearity to compute the output by combining the response to the individual frequencies. A sample frequency response is shown in Figure 3.2b.

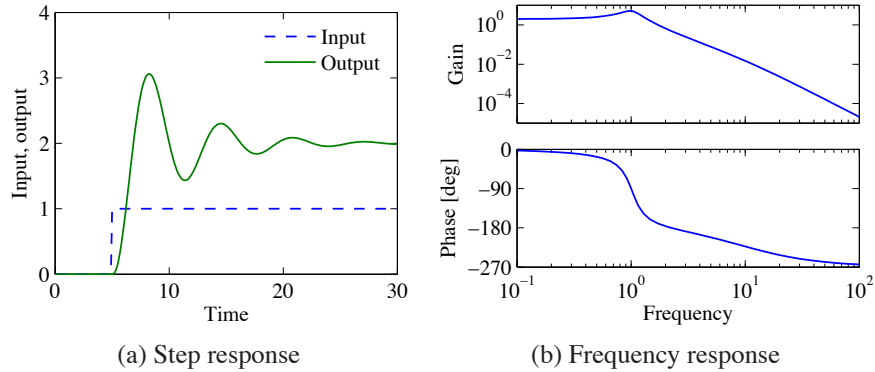(a) Step response   (b) Frequency response

Figure 3.2: Input/output response of a linear system. The step response (a) shows the output of the system due to an input that changes from 0 to 1 at time $t = 5$ s. The frequency response (b) shows the amplitude gain and phase change due to a sinusoidal input at different frequencies.

The input/output view lends itself naturally to experimental determination of system dynamics, where a system is characterized by recording its response to particular inputs, e.g., a step or a set of sinusoids over a range of frequencies.

The Control View

When control theory emerged as a discipline in the 1940s, the approach to dynamics was strongly influenced by the electrical engineering (input/output) view. A second wave of developments in control, starting in the late 1950s, was inspired by mechanics, where the state space perspective was used. The emergence of space flight is a typical example, where precise control of the orbit of a spacecraft is essential. These two points of view gradually merged into what is today the state space representation of input/output systems.

The development of state space models involved modifying the models from mechanics to include external actuators and sensors and utilizing more general forms of equations. In control, the model given by equation (**??**) was replaced by

$$\frac{dx}{dt} = f(x, u), \qquad y = h(x, u), \tag{3.1}$$

where x is a vector of state variables, u is a vector of control signals and y is a vector of measurements. The term dx/dt represents the derivative of x with respect to time, now considered a vector, and f and h are (possibly nonlinear) mappings of their arguments to vectors of the appropriate dimension. For mechanical systems, the state consists of the position and velocity of the system, so that $x = (q, \dot{q})$ in the case of a damped spring–mass system. Note that in the control formulation we model dynamics as first-order differential equations, but we will see that this can

capture the dynamics of higher-order differential equations by appropriate definition of the state and the maps f and h.

Adding inputs and outputs has increased the richness of the classical problems and led to many new concepts. For example, it is natural to ask if possible states x can be reached with the proper choice of u (reachability) and if the measurement y contains enough information to reconstruct the state (observability). These topics will be addressed in greater detail in Chapters **??** and **??**.

A final development in building the control point of view was the emergence of disturbances and model uncertainty as critical elements in the theory. The simple way of modeling disturbances as deterministic signals like steps and sinusoids has the drawback that such signals cannot be predicted precisely. A more realistic approach is to model disturbances as random signals. This viewpoint gives a natural connection between prediction and control. The dual views of input/output representations and state space representations are particularly useful when modeling uncertainty since state models are convenient to describe a nominal model but uncertainties are easier to describe using input/output models (often via a frequency response description). Uncertainty will be a constant theme throughout the text and will be studied in particular detail in Chapter **??**.

An interesting observation in the design of control systems is that feedback systems can often be analyzed and designed based on comparatively simple models. The reason for this is the inherent robustness of feedback systems. However, other uses of models may require more complexity and more accuracy. One example is feedforward control strategies, where one uses a model to precompute the inputs that cause the system to respond in a certain way. Another area is system validation, where one wishes to verify that the detailed response of the system performs as it was designed. Because of these different uses of models, it is common to use a hierarchy of models having different complexity and fidelity.

State space systems

The state of a system is a collection of variables that summarize the past of a system for the purpose of predicting the future. For a biochemical system the state is composed of the variables required to account for the current context of the cell, including the concentrations of the various species and complexes that are present. It may also include the spatial locations of the various molecules. A key issue in modeling is to decide how accurately this information has to be represented. The state variables are gathered in a vector $x \in \mathbb{R}^n$ called the *state vector*. The control variables are represented by another vector $u \in \mathbb{R}^p$, and the measured signal by the vector $y \in \mathbb{R}^q$. A system can then be represented by the differential equation

$$\frac{dx}{dt} = f(x, u), \qquad y = h(x, u), \tag{3.2}$$

where $f : \mathbb{R}^n \times \mathbb{R}^p \to \mathbb{R}^n$ and $h : \mathbb{R}^n \times \mathbb{R}^p \to \mathbb{R}^q$ are smooth mappings. We call a model of this form a *state space model*.

The dimension of the state vector is called the *order* of the system. The system (3.2) is called *time-invariant* because the functions f and h do not depend explicitly on time t; there are more general time-varying systems where the functions do depend on time. The model consists of two functions: the function f gives the rate of change of the state vector as a function of state x and control u, and the function h gives the measured values as functions of state x and control u.

A system is called a *linear* state space system if the functions f and h are linear in x and u. A linear state space system can thus be represented by

$$\frac{dx}{dt} = Ax + Bu, \qquad y = Cx + Du, \tag{3.3}$$

where A, B, C and D are constant matrices. Such a system is said to be *linear and time-invariant*, or LTI for short. The matrix A is called the *dynamics matrix*, the matrix B is called the *control matrix*, the matrix C is called the *sensor matrix* and the matrix D is called the *direct term*. Frequently systems will not have a direct term, indicating that the control signal does not influence the output directly.

3.2 Analysis Near Equilibria

As in the case of many other classes of dynamical systems, a great deal of insight into the behavior of a biological system can be obtained by analyzing the dynamics of the system subject to small perturbations around a known solution. We begin by considering the dynamics of the system near an equilibrium point, which is one of the simplest cases and provides a rich set of methods and tools.

In this section we will model the dynamics of our system using a nonlinear ordinary differential equation of the form

$$\dot{x} = f(x, \theta, w), \qquad y = h(x, \theta) \tag{3.4}$$

where $x \in \mathbb{R}^n$ is the system state, $\theta \in \mathbb{R}^K$ are the system parameters and $w \in \mathbb{R}^p$ is a set of external inputs. The output y of the system represents quantities that can be measured or that are used to interconnect subsystem models to form larger models. Note that we have chosen to explicitly model the system parameters θ, which can be thought of as an additional set of (mainly constant) inputs to the system.

Equilibrium points and stability [AM08]

We begin by considering the case where the input w and parameters θ in equation (3.4) are fixed and hence we can write the dynamics of the system as

$$\frac{dx}{dt} = F(x).$$
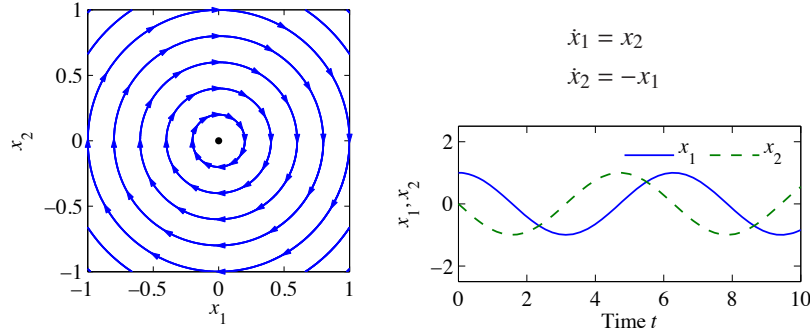
$$\dot{x}_1 = x_2$$
$$\dot{x}_2 = -x_1$$

Figure 3.3: Phase portrait and time domain simulation for a system with a single stable equilibrium point. The equilibrium point x_e at the origin is stable since all trajectories that start near x_e stay near x_e.

An *equilibrium point* of a dynamical system represents a stationary condition for the dynamics. We say that a state x_e is an equilibrium point for a dynamical system if $F(x_e) = 0$. If a dynamical system has an initial condition $x(0) = x_e$, then it will stay at the equilibrium point: $x(t) = x_e$ for all $t \geq 0$, where we have taken $t_0 = 0$.

Equilibrium points are one of the most important features of a dynamical system since they define the states corresponding to constant operating conditions. A dynamical system can have zero, one or more equilibrium points.

The *stability* of an equilibrium point determines whether or not solutions nearby the equilibrium point remain close, get closer or move further away. An equilibrium point x_e is *stable* if solutions that start near x_e stay close to x_e. Formally, we say that the equilibrium point x_e is stable if for all $\epsilon > 0$, there exists a $\delta > 0$ such that

$$\|x(0) - x_e\| < \delta \quad \implies \quad \|x(t) - x_e\| < \epsilon \quad \text{for all } t > 0,$$

where $x(t)$ represents the solution the the differential equation (**??**) with initial condition $x(0)$. Note that this definition does not imply that $x(t)$ approaches x_e as time increases but just that it stays nearby. Furthermore, the value of δ may depend on ϵ, so that if we wish to stay very close to the solution, we may have to start very, very close ($\delta \ll \epsilon$). This type of stability, which is illustrated in Figure **??**, is also called *stability in the sense of Lyapunov*. If an equilibrium point is stable in this sense and the trajectories do not converge, we say that the equilibrium point is *neutrally stable*.

An example of a neutrally stable equilibrium point is shown in Figure 3.3. From the phase portrait, we see that if we start near the equilibrium point, then we stay near the equilibrium point. Indeed, for this example, given any ϵ that defines the range of possible initial conditions, we can simply choose $\delta = \epsilon$ to satisfy the definition of stability since the trajectories are perfect circles.

An equilibrium point x_e is *asymptotically stable* if it is stable in the sense of
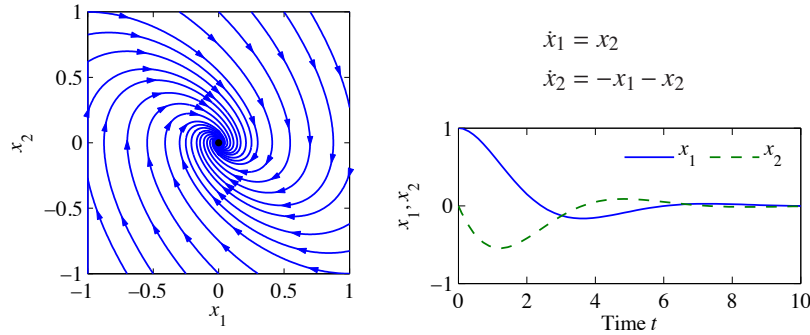
$$\dot{x}_1 = x_2$$
$$\dot{x}_2 = -x_1 - x_2$$

Figure 3.4: Phase portrait and time domain simulation for a system with a single asymptotically stable equilibrium point. The equilibrium point x_e at the origin is asymptotically stable since the trajectories converge to this point as $t \to \infty$.

Lyapunov and also $x(t) \to x_e$ as $t \to \infty$ for $x(0)$ sufficiently close to x_e. This corresponds to the case where all nearby trajectories converge to the stable solution for large time. Figure 3.4 shows an example of an asymptotically stable equilibrium point. Note from the phase portraits that not only do all trajectories stay near the equilibrium point at the origin, but that they also all approach the origin as t gets large (the directions of the arrows on the phase portrait show the direction in which the trajectories move).

An equilibrium point x_e is *unstable* if it is not stable. More specifically, we say that an equilibrium point x_e is unstable if given some $\epsilon > 0$, there does *not* exist a $\delta > 0$ such that if $\|x(0) - x_e\| < \delta$, then $\|x(t) - x_e\| < \epsilon$ for all t. An example of an unstable equilibrium point is shown in Figure 3.5.

The definitions above are given without careful description of their domain of applicability. More formally, we define an equilibrium point to be *locally stable* (or *locally asymptotically stable*) if it is stable for all initial conditions $x \in B_r(a)$, where

$$B_r(a) = \{x : \|x - a\| < r\}$$

is a ball of radius r around a and $r > 0$. A system is *globally stable* if it is stable for all $r > 0$. Systems whose equilibrium points are only locally stable can have interesting behavior away from equilibrium points, as we explore in the next section.

To better understand the dynamics of the system, we can examine the set of all initial conditions that converge to a given asymptotically stable equilibrium point. This set is called the *region of attraction* for the equilibrium point. In general, computing regions of attraction is difficult. However, even if we cannot determine the region of attraction, we can often obtain patches around the stable equilibria that are attracting. This gives partial information about the behavior of the system.

For planar dynamical systems, equilibrium points have been assigned names based on their stability type. An asymptotically stable equilibrium point is called
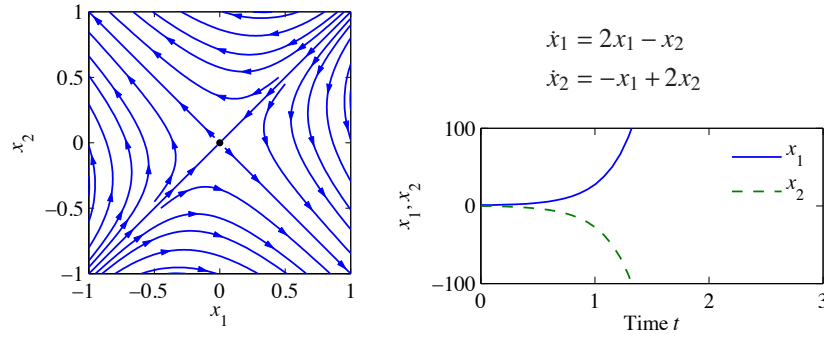
$$\dot{x}_1 = 2x_1 - x_2$$
$$\dot{x}_2 = -x_1 + 2x_2$$

Figure 3.5: Phase portrait and time domain simulation for a system with a single unstable equilibrium point. The equilibrium point x_e at the origin is unstable since not all trajectories that start near x_e stay near x_e. The sample trajectory on the right shows that the trajectories very quickly depart from zero.

a *sink* or sometimes an *attractor*. An unstable equilibrium point can be either a *source*, if all trajectories lead away from the equilibrium point, or a *saddle*, if some trajectories lead to the equilibrium point and others move away (this is the situation pictured in Figure 3.5). Finally, an equilibrium point that is stable but not asymptotically stable (i.e., neutrally stable, such as the one in Figure 3.3) is called a *center*.

Stability analysis via linearization

A linear dynamical system has the form

$$\frac{dx}{dt} = Ax, \quad x(0) = x_0, \tag{3.5}$$

where $A \in \mathbb{R}^{n \times n}$ is a square matrix, corresponding to the dynamics matrix of a linear control system (**??**). For a linear system, the stability of the equilibrium at the origin can be determined from the eigenvalues of the matrix A:

$$\lambda(A) = \{s \in \mathbb{C} : \det(sI - A) = 0\}.$$

The polynomial $\det(sI - A)$ is the *characteristic polynomial* and the eigenvalues are its roots. We use the notation λ_j for the jth eigenvalue of A, so that $\lambda_j \in \lambda(A)$. In general λ can be complex-valued, although if A is real-valued, then for any eigenvalue λ, its complex conjugate λ^* will also be an eigenvalue. The origin is always an equilibrium for a linear system. Since the stability of a linear system depends only on the matrix A, we find that stability is a property of the system. For a linear system we can therefore talk about the stability of the system rather than the stability of a particular solution or equilibrium point.

The easiest class of linear systems to analyze are those whose system matrices are in diagonal form. In this case, the dynamics have the form

$$
\frac{dx}{dt} = \begin{pmatrix} \lambda_1 & & & 0 \\ & \lambda_2 & & \\ & & \ddots & \\ 0 & & & \lambda_n \end{pmatrix} x. \tag{3.6}
$$

It is easy to see that the state trajectories for this system are independent of each other, so that we can write the solution in terms of n individual systems $\dot{x}_j = \lambda_j x_j$. Each of these scalar solutions is of the form

$$
x_j(t) = e^{\lambda_j t} x_j(0).
$$

We see that the equilibrium point $x_e = 0$ is stable if $\lambda_j \leq 0$ and asymptotically stable if $\lambda_j < 0$.

Another simple case is when the dynamics are in the block diagonal form

$$
\frac{dx}{dt} = \begin{pmatrix} \sigma_1 & \omega_1 & & 0 & 0 \\ -\omega_1 & \sigma_1 & & 0 & 0 \\ 0 & 0 & \ddots & \vdots & \vdots \\ 0 & 0 & & \sigma_m & \omega_m \\ 0 & 0 & & -\omega_m & \sigma_m \end{pmatrix} x.
$$

In this case, the eigenvalues can be shown to be $\lambda_j = \sigma_j \pm i\omega_j$. We once again can separate the state trajectories into independent solutions for each pair of states, and the solutions are of the form

$$
x_{2j-1}(t) = e^{\sigma_j t}(x_{2j-1}(0)\cos\omega_j t + x_{2j}(0)\sin\omega_j t),
$$
$$
x_{2j}(t) = e^{\sigma_j t}(-x_{2j-1}(0)\sin\omega_j t + x_{2j}(0)\cos\omega_j t),
$$

where $j = 1, 2, \ldots, m$. We see that this system is asymptotically stable if and only if $\sigma_j = \mathrm{Re}\,\lambda_j < 0$. It is also possible to combine real and complex eigenvalues in (block) diagonal form, resulting in a mixture of solutions of the two types.

Very few systems are in one of the diagonal forms above, but some systems can be transformed into these forms via coordinate transformations. One such class of systems is those for which the dynamics matrix has distinct (non-repeating) eigenvalues. In this case there is a matrix $T \in \mathbb{R}^{n \times n}$ such that the matrix TAT^{-1} is in (block) diagonal form, with the block diagonal elements corresponding to the eigenvalues of the original matrix A (see Exercise ??). If we choose new coordinates $z = Tx$, then

$$
\frac{dz}{dt} = T\dot{x} = TAx = TAT^{-1}z
$$

and the linear system has a (block) diagonal dynamics matrix. Furthermore, the eigenvalues of the transformed system are the same as the original system since

if v is an eigenvector of A, then $w = Tv$ can be shown to be an eigenvector of TAT^{-1}. We can reason about the stability of the original system by noting that $x(t) = T^{-1}z(t)$, and so if the transformed system is stable (or asymptotically stable), then the original system has the same type of stability.

This analysis shows that for linear systems with distinct eigenvalues, the stability of the system can be completely determined by examining the real part of the eigenvalues of the dynamics matrix. For more general systems, we make use of the following theorem, proved in the next chapter:

Theorem 3.1 (Stability of a linear system). *The system*

$$\frac{dx}{dt} = Ax$$

is asymptotically stable if and only if all eigenvalues of A all have a strictly negative real part and is unstable if any eigenvalue of A has a strictly positive real part.

An important feature of differential equations is that it is often possible to determine the local stability of an equilibrium point by approximating the system by a linear system. Suppose that we have a nonlinear system

$$\frac{dx}{dt} = F(x)$$

that has an equilibrium point at x_e. Computing the Taylor series expansion of the vector field, we can write

$$\frac{dx}{dt} = F(x_e) + \left.\frac{\partial F}{\partial x}\right|_{x_e} (x - x_e) + \text{higher-order terms in } (x - x_e).$$

Since $F(x_e) = 0$, we can approximate the system by choosing a new state variable $z = x - x_e$ and writing

$$\frac{dz}{dt} = Az, \qquad \text{where} \quad A = \left.\frac{\partial F}{\partial x}\right|_{x_e}. \tag{3.7}$$

We call the system (3.7) the *linear approximation* of the original nonlinear system or the *linearization* at x_e.

The fact that a linear model can be used to study the behavior of a nonlinear system near an equilibrium point is a powerful one. Indeed, we can take this even further and use a local linear approximation of a nonlinear system to design a feedback law that keeps the system near its equilibrium point (design of dynamics). Thus, feedback can be used to make sure that solutions remain close to the equilibrium point, which in turn ensures that the linear approximation used to stabilize it is valid.

Input/output transfer curves (TBD)

Frequency domain analysis

Another way to look at the sensitivity of the solutions near equilibria to changes in parameters and inputs is to use frequency domain techniques. Recall that the *frequency response* of a linear system

$$\dot{x} = Ax + Bu$$
$$y = Cx + Du$$

is the response of the system to a sinusoidal input $u = a\sin\omega t$ with input amplitude a and frequency ω. The transfer function for a linear system is given by

$$G_{yu}(s) = C(sI - A)^{-1}B + D$$

and represents the response of a system to an exponential signal of the form $u(t) = e^{st}$ where $s \in \mathbb{C}$. In particular, the response to a sinusoid $u = a\sin\omega t$ is given by $y = Ma\sin(\omega t + \theta)$ where the gain M and phase shift θ can be determined from the transfer function evaluated at $s = i\omega$:

$$G_{yu}(i\omega) = Me^{i\theta}.$$

For finite dimensional linear (or linearized) systems, the transfer function be be written as a ratio of polynomials in s:

$$G(s) = \frac{b(s)}{a(s)}.$$

The values of s at which the numerator vanishes are called the zeros of the transfer function and the values of s at which the denominator vanishes are called the poles.

The transfer function representation of an input/output linear system is essentially equivalent to the state space description, but we reason about the dynamics by looking at the transfer function instead of the state space matrices. For example, it can be shown that the poles of a transfer function correspond to the eigenvalues of the matrix A, and hence the poles determine the stability of the system.

Interconnections between subsystems often have simple representations in terms of transfer functions. Two systems G_1 and G_2 in series (with the output of the first connected to the input of the second) have a combined transfer function $G_{\text{series}}(s) = G_1(s)G_2(s)$ and two systems in parallel (a single input goes to both systems and the outputs are summed) has the transfer function $G_{\text{parallel}}(s) = G_1(s) + G_2(s)$. A common interconnection is two put two systems in feedback form for which the transfer function is given by

$$G_{yr}(s) = \frac{G_1(s)}{G_1(s) + G_2(s)} = \frac{n_1(s)d_2(s)}{n_1(s)d_2(s) + d_1(s)n_2(s)},$$

where $n_i(s)$ and $d_i(s)$ are the numerator and denominator of the individual transfer function. The ease in which the input/output response for interconnected systems can be computed with transfer functions is one of the main motivations for their widespread use in engineering.

Transfer functions are useful representations of linear systems because the properties of the transfer function can be related to the properties of the dynamics. In particular, the shape of the frequency response describes how the system response to inputs and disturbances, as well as allows us to reason about the stability of interconnected systems. The Bode plot of a transfer function gives the magnitude and phase of the frequency response as a function of frequency and the Nyquist plot can be used to reason about stability of a closed loop system from the open loop frequency response. The transfer function for a system can be determined from experiments by measuring the frequency response and fitting a transfer function to the data. Formally, the transfer function corresponds to the ratio of the Laplace transforms of the output to the input.

Returning to our analysis of biomolecular systems, suppose we have a systems whose dynamics can be written as

$$\dot{x} = f(x, \theta, w)$$

and we wish to understand how the solutions of the system depend on the parameters θ and disturbances w. We focus on the case of an equilibrium solution $x(t; x_0, \theta_0) = x_e$. Let $z = x - x_e$, $\tilde{w} = w - w_0$ and $\tilde{\theta} = \theta - \theta_0$ represent the deviation of the state, input and parameters from their nominal values. We can write the dynamics of the perturbed system using its linearization:

$$\frac{dz}{dt} = \left(\frac{\partial f}{\partial x}\right)_{(x_e, \theta_0, w_0)} \cdot z \quad + \quad \left(\frac{\partial f}{\partial \theta}\right)_{(x_e, \theta_0, w_0)} \cdot \tilde{\theta} \quad + \quad \left(\frac{\partial f}{\partial w}\right)_{(x_e, \theta_0, w_0)} \cdot \tilde{w}.$$

This linear system describes small deviations from $x_e(\theta_0, w_0)$ but allows $\tilde{\theta}$ and $\tilde{w}$ to be time-varying instead of the constant case considered earlier.

To analyze the resulting deviations, it is convenient to look at the system in the frequency domain. Let $y = Cx$ be a set of values of interest. The transfer functions between $\tilde{\theta}$, $\tilde{w}$ and y are given by

$$H_{y\tilde{\theta}}(s) = C(sI - A)^{-1}B_\theta, \qquad H_{y\tilde{w}}(s) = C(sI - A)^{-1}B_w,$$

where

$$A = \frac{\partial f}{\partial x}\bigg|_{(x_e, \theta_0, w_0)}, \qquad B_\theta = \frac{\partial f}{\partial \theta}\bigg|_{(x_e, \theta_0, w_0)}, \qquad B_w = \frac{\partial f}{\partial w}\bigg|_{(x_e, \theta_0, w_0)}.$$

Note that if we let $s = 0$, we get the response to small, constant changes in parameters. For example, the change in the outputs y as a function of constant changes in the parameters is given by

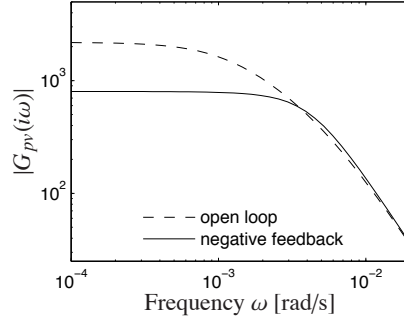$$H_{y\tilde{\theta}}(0) = CA^{-1}B_\theta = CS_{x,\theta},$$

Figure 3.6: Noise attenuation in a genetic circuit.

which matches our previous parametric analysis.

Example 3.1 (Transcriptional regulation)**.** Consider again the case of transcriptional regulation described in Example 3.2. Suppose that the mRNA degradation rate γ can change as a function of time and that we wish to understand the sensitivity with respect to this (time-varying) parameter. Linearizing the dynamics around an equilibrium point

$$A = \begin{pmatrix} -\gamma & F'(p_e) \\ \beta & -\delta \end{pmatrix}, \qquad B_\gamma = \begin{pmatrix} -m_e \\ 0 \end{pmatrix}.$$

For the case of no feedback we have $F(P) = \alpha_0$, and the system has an equilibrium point at $m_e = \alpha_0/\gamma$, $P_e = \beta\alpha_0/(\delta\gamma)$. The transfer function from γ to p is given by

$$G_{P\gamma}^{\mathrm{ol}}(s) = \frac{-\beta m_e}{(s+\gamma)(s+\delta)}.$$

For the case of negative regulation, we have

$$F(P) = \frac{\alpha}{K+P^n} + \alpha_0,$$

and the resulting transfer function is given by

$$G_{P\gamma}^{\mathrm{cl}}(s) = \frac{\beta m_e}{(s+\gamma)(s+\delta)+\beta\sigma}, \qquad \sigma = F'(P_e) = \frac{n\alpha P_e^{n-1}}{(K+P_e^n)^2}.$$

Figure 3.6 shows the frequency response for the two circuits. We see that the feedback circuit attenuates the response of the system to disturbances with low-frequency content but slightly amplifies disturbances at high frequency (compared to the open loop system). ∇

3.3 Robustness

Disturbance rejection

Parametric uncertainty

In addition to studying the input/output transfer curve and the stability of a given equilibrium points, we can also study how these features change with respect to changes in the system parameters θ. Let $x_e(\theta_0, w_0)$ represent an equilibrium point for fixed parameters θ_0 and external input w_0, so that $f(x_e, \theta_0, w_0) = 0$. We assume that the equilibrium point is stable and focus here on understanding how the location of the equilibrium point and the dynamics near the equilibrium point vary as a function of changes in the parameters θ and external inputs w.

We start by assuming that $w = 0$ and investigating how x_e depends on θ. The simplest approach is to analytically solve the equation $f(x_e, \theta_0) = 0$ for x_e. However, this is often difficult to do in closed form and so as an alternative we instead look at the linearized response given by $S_{x_e\theta} = dx_e/d\theta$, the (infinitesimal) change in the equilibrium state due to a change in the parameter. To determine $S_{x_e\theta}$ we begin by differentiating the relationship $f(x_e(\theta), \theta) = 0$ with respect to θ:

$$\frac{df}{d\theta} = \frac{\partial f}{\partial x}\frac{\partial x_e}{\partial \theta} + \frac{\partial f}{\partial \theta} = 0 \quad \implies \quad \frac{\partial x_e}{\partial \theta} = -\left(\frac{\partial f}{\partial x}\right)^{-1}\frac{\partial f}{\partial \theta}\bigg|_{(xe,\theta_0)}. \tag{3.8}$$

These quantities can be computed numerically and hence we can evaluate the effect of small (but constant) changes in the parameters θ on the equilibrium state x_e.

A similar analysis can be performed to determine the effects of small (but constant) changes in the external input w. Suppose that x_e depends on both θ and w, with $f(x_e, \theta_0, w_0) = 0$ and θ_0 and w_0 representing the nominal values. Then

$$\frac{\partial x_e}{\partial \theta} = -\left(\frac{\partial f}{\partial x}\right)^{-1}\frac{\partial f}{\partial \theta}\bigg|_{(xe,\theta_0,w_0)}, \qquad \frac{\partial x_e}{\partial w} = -\left(\frac{\partial f}{\partial x}\right)^{-1}\frac{\partial f}{\partial w}\bigg|_{(xe,\theta_0,w_0)}.$$

We see that the vector $\partial f/\partial w$ describes how the specific inputs vary and $(\partial f/\partial x)^{-1}$ indicates how the perturbations are reflected in the equilibrium states. If the system is close to instability then some eigenvalues of $\partial f/\partial x$ may be near zero and hence the inverse could be large, resulting in significant changes in the equilibrium point due to variations in the disturbances (or parameters).

Example 3.2 (Transcriptional regulation). Consider a genetic circuit consisting of a single gene. We wish to study the response of the protein concentration to fluctuations in its parameters in two cases: a *constitutive promoter* (no regulation) and self-repression (negative feedback), illustrated in Figure 3.7. The dynamics of the system are given by

$$\frac{dm}{dt} = F(P) - \gamma m, \qquad \frac{dP}{dt} = \beta m - \delta P,$$
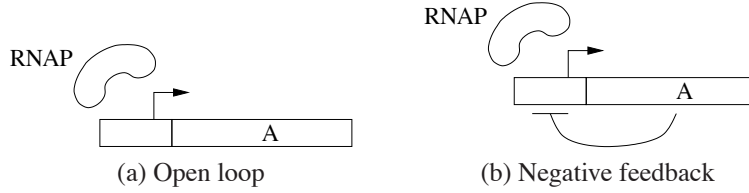
(a) Open loop

(b) Negative feedback

Figure 3.7: Parameter sensitivity in a genetic circuit. The open loop system (a) consists of a constitutive promoter, while the closed loop circuit (b) is self-regulated with negative feedback (repressor).

where m is the mRNA concentration and P is the protein concentration.

For the case of no feedback we have $F(p) = \alpha_0$, and the system has an equilibrium point at $m_e = \alpha_0/\gamma$, $P_e = \beta\alpha_0/(\delta\gamma)$. The parameter vector can be taken as $\theta = (\alpha_0, \gamma, \beta, \delta)$. Since we have a simple expression for the equilibrium concentrations, we can compute the sensitivity to the parameters directly:

$$\frac{\partial x_e}{\partial \theta} = \begin{pmatrix} \frac{1}{\gamma} & -\frac{\alpha_0}{\gamma^2} & 0 & 0 \\ \frac{\beta}{\delta\gamma} & -\frac{\beta\alpha_0}{\delta\gamma^2} & \frac{\alpha_0}{\delta\gamma} & -\frac{\beta\alpha_0}{\gamma\delta^2} \end{pmatrix},$$

where the parameters are evaluated at their nominal values, but we leave off the subscript 0 on the individual parameters for simplicity. If we choose the parameters as $\theta_0 = (0.00138, 0.00578, 0.115, 0.00116)$, then the resulting sensitivity matrix evaluates to

$$S^{\text{open}}_{x_e,\theta} \approx \begin{pmatrix} 170 & -41 & 0 & 0 \\ 17000 & -4100 & 210 & -21000 \end{pmatrix}. \tag{3.9}$$

If we look instead at the scaled sensitivity matrix, then the open loop nature of the system yields a particularly simple form:

$$\bar{S}^{\text{open}}_{x_e,\theta} = \begin{pmatrix} 1 & -1 & 0 & 0 \\ 1 & -1 & 1 & -1 \end{pmatrix}. \tag{3.10}$$

In other words, a 10% change in any of the parameters will lead to a comparable positive or negative change in the equilibrium values.

For the case of negative regulation, we have

$$F(P) = \frac{\alpha}{K + P^n} + \alpha_0,$$

and the equilibrium points satisfy

$$m_e = \frac{\delta}{\beta}P_e, \qquad \frac{\alpha}{K + P_e^n} + \alpha_0 = \gamma m_e = \frac{\gamma\delta}{\beta}P_e. \tag{3.11}$$

In order to make a proper comparison with the previous case, we need to be careful to choose the parameters so that the equilibrium concentration P_e matches that of

the open look system. We can do this by modifying the promoter strength α or the RBS strength β so that the second formula in equation (3.11) is satisfied or, equivalently, choose the parameters for the open loop case so that they match the closed loop steady state protein concentration.

Rather than attempt to solve for the equilibrium point in closed form, we instead investigate the sensitivity using the computations in equation (3.8). The state, dynamics and parameters are given by

$$x = \begin{pmatrix} m & P \end{pmatrix}, \qquad f(x,\theta) = \begin{pmatrix} F(P) - \gamma m \\ \beta m - \delta P \end{pmatrix}, \qquad \theta = \begin{pmatrix} \alpha_0 & \gamma & \beta & \delta & \alpha & n & K \end{pmatrix}.$$

Note that the parameters are ordered such that the first four parameters match the open loop system. The linearizations are given by

$$\frac{\partial f}{\partial x} = \begin{pmatrix} -\gamma & F'(P_e) \\ \beta & -\delta \end{pmatrix}, \qquad \frac{\partial f}{\partial \theta} = \begin{pmatrix} 1 & -m & 0 & 0 & \frac{1}{K+P^n} & \frac{\alpha P^n \log(P)}{(K+P^n)^2} & \frac{\alpha}{(K+P^n)^2} \\ 0 & 0 & m & -P & 0 & 0 & 0 \end{pmatrix},$$

where again the parameters are taken to be their nominal values. From this we can compute the sensitivity matrix as

$$S_{x,\theta} = \begin{pmatrix} -\frac{\delta \frac{\partial \alpha}{\partial \alpha_0}}{\delta\gamma - \beta F'} & \frac{\delta m}{\delta\gamma - \beta F'} & -\frac{mF'}{\delta\gamma - \beta F'} & \frac{PF'}{\delta\gamma - \beta F'} & -\frac{\delta \frac{\partial \alpha}{\partial \alpha_1}}{\delta\gamma - \beta F'} & -\frac{\delta \frac{\partial \alpha}{\partial n}}{\delta\gamma - \beta F'} & -\frac{\delta \frac{\partial \alpha}{\partial K}}{\delta\gamma - \beta F'} \\ -\frac{\beta \frac{\partial \alpha}{\partial \alpha_0}}{\delta\gamma - \beta F'} & \frac{\beta m}{\delta\gamma - \beta F'} & -\frac{\gamma m}{\delta\gamma - \beta F'} & \frac{\gamma P}{\delta\gamma - \beta F'} & -\frac{\beta \frac{\partial \alpha}{\partial \alpha_1}}{\delta\gamma - \beta F'} & -\frac{\beta \frac{\partial \alpha}{\partial n}}{\delta\gamma - \beta F'} & -\frac{\beta \frac{\partial \alpha}{\partial K}}{\delta\gamma - \beta F'} \end{pmatrix},$$

where $F' = \partial F/\partial P$ and all other derivatives of F are evaluated at the nominal parameter values.

We can now evaluate the sensitivity at the same protein concentration as we use in the open loop case. The equilibrium point is given by

$$x_e = \begin{pmatrix} m_e \\ P_e \end{pmatrix} = \begin{pmatrix} \frac{\alpha_0}{\gamma} \\ \frac{\alpha_0 \beta}{\delta \gamma} \end{pmatrix} = \begin{pmatrix} 0.239 \\ 23.9 \end{pmatrix}$$

and the sensitivity matrix is

$$S_{x_e,\theta}^{closed} \approx \begin{pmatrix} 76.1 & -18.2 & -1.16 & 116. & 0.134 & -0.212 & -0.000117 \\ 7610. & -1820. & 90.8 & -9080. & 13.4 & -21.2 & -0.0117 \end{pmatrix}.$$

The scaled sensitivity matrix becomes

$$\bar{S}_{x_e,\theta}^{closed} \approx \begin{pmatrix} 0.16 & -0.44 & -0.56 & 0.56 & 0.28 & -1.78 & -3.08 \times 10^{-7} \\ 0.16 & -0.44 & 0.44 & -0.44 & 0.28 & -1.78 & -3.08 \times 10^{-7} \end{pmatrix}. \quad (3.12)$$

Comparing this equation with equation (3.10), we see that there is reduction in the sensitivity with respect to most parameters. In particular, we become less sensitive to those parameters that are not part of the feedback (columns 2–4), but there is higher sensitivity with respect to some of the parameters that are part of the feedback mechanisms (particularly n). $\qquad\qquad \nabla$

More generally, we may wish to evaluate the sensitivity of a (non-constant) solution to parameter changes. This can be done by computing the function $dx(t)/d\theta$, which describes how the state changes at each instant in time as a function of (small) changes in the parameters θ. We assume $w = 0$ for simplicity of exposition.

Let $x(t; x_0, \theta_0)$ be a solution of the dynamics with initial condition x_0 and parameters θ_0. To compute $dx/d\theta$, we write down a differential equation for how it evolves in time:

$$\frac{d}{dt}\left(\frac{dx}{d\theta}\right) = \frac{d}{d\theta}\left(\frac{dx}{dt}\right) = \frac{d}{d\theta}(f(x,\theta,w))$$
$$= \frac{\partial f}{\partial x}\frac{dx}{d\theta} + \frac{\partial f}{\partial \theta}.$$

This is a differential equation with $n \times m$ states $S_{ij} = dx_i/d\theta_j$ and with initial condition $S_{ij}(0) = 0$ (since changes to the parameters to not affect the initial conditions).

To solve these equations, we must simultaneously solve for the state x and the sensitivity S (whose dynamics depend on x). Thus, we must solve the set of $n + nm$ coupled differential equations

$$\frac{dx}{dt} = f(x,\theta,w), \qquad \frac{dS_{x\theta}}{dt} = \frac{\partial f}{\partial x}(x,\theta,w)S_{x\theta} + \frac{\partial f}{\partial \theta}(x,\theta,w). \qquad (3.13)$$

This differential equation generalizes our previous results by allowing us to evaluate the sensitivity around a (non-constant) trajectory. Note that in the special case that we are at an equilibrium point and the dynamics for $S_{x,\theta}$ are stable, the steady state solution of equation (3.13) is identical to that obtained in equation (3.8). However, equation (3.13) is much more general, allowing us to determine the change in the state of the system at a fixed time T, for example. This equation also does not require that our solution stay near an equilibrium point, it only requires that our perturbations in the parameters are sufficiently small.

Example 3.3 (Repressilator). Consider the example of the repressilator, which was described in Example 2.4. The dynamics of this system can be written as

$$\frac{dm_1}{dt} = F_{\text{rep}}(P_3) - \gamma m_1 \qquad \frac{dP_1}{dt} = \beta m_1 - \delta P_1$$
$$\frac{dm_2}{dt} = F_{\text{rep}}(P_1) - \gamma m_2 \qquad \frac{dP_2}{dt} = \beta m_2 - \delta P_2$$
$$\frac{dm_3}{dt} = F_{\text{rep}}(P_2) - \gamma m_2 \qquad \frac{dP_3}{dt} = \beta m_3 - \delta P_2,$$

where the repressor is modeled using a Hill function

$$F_{\text{rep}}(p) = \frac{\alpha}{K + p^n} + \alpha_0.$$

The dynamics of this system lead to a limit cycle in the protein concentrations, as shown in Figure 3.8a.

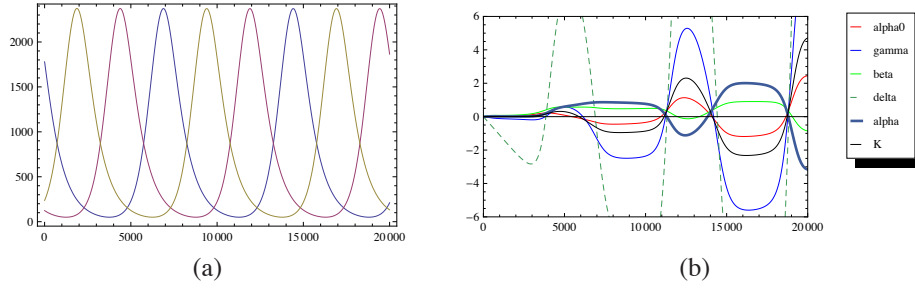| (a) | (b) |

Figure 3.8: Repressilator sensitivity plots

We can analyze the sensitivity of the protein concentrations to changes in the parameters using the sensitivity differential equation. Since our solution is periodic, the sensitivity dynamics will satisfy an equation of the form

$$\frac{dS_{x,\theta}}{dt} = A(t)S_{x,\theta} + B(t),$$

where $A(t)$ and $B(t)$ are both periodic in time. Letting $x = (m_1, P_1, m_2, P_2, m_3, P_3)$ and $\theta = (\alpha_0, \gamma, \beta, \delta, \alpha, K)$, we can compute $S_{x,\theta}$ along the limit cycle. If the dynamics for $S_{x,\theta}$ are stable then the resulting solutions will be periodic, showing how the dynamics around the limit cycle depend on the parameter values. The results are shown in Figure 3.8b, where we plot the steady state sensitivity of P_1 as a function of time. We see, for example, that the limit cycle depends strongly on the protein degradation and dilution rate γ, indicating that changes in this value can lead to (relatively) large variations in the magnitude of the limit cycle.

∇

Several simulation tools include the ability to do sensitivity analysis of this sort, including COPASI.

Unmodeled dynamics

A slightly more general analysis of sensitivity can be accomplished using the control theoretic notions of sensitivity described in AM08, Chapter 12. Rather than just considering static changes to parameter values, we can instead consider the case of *unmodeled dynamics*, in which we allow bounded input/output uncertainties to enter the system dynamics. This can be used to model parameters whose values are unknown and also time-varying, as well as capturing uncertain dynamics that are being ignored or approximated.

To illustrate the basic approach, consider the problem of determining the sensitivity of a set of reactions to a set of additional unmodeled reactions, whose detailed effects are unknown but assumed to be bounded. We set this problem up using the general framework shown in Figure 3.9.
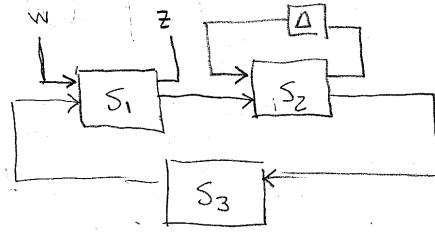
Figure 3.9: Analysis of dynamic uncertainty in a reaction system.

3.4 Analysis of Reaction Rate Equations

The previous section considered analysis techniques for general dynamical systems with small perturbations. In this section, we specialize to the case where the dynamics have the form of a reaction rate equation:

$$\dot{x} = Nv(x,\theta), \tag{3.14}$$

where x is the vector of species concentrations, θ is the vector of reaction parameters, N is the stoichiometry matrix and $v(x,\theta)$ is the reaction rate (or flux) vector.

Reduced reaction dynamics

When analyzing reaction rate equations, it is often the case that there are conserved quantities in the dynamics. For example, conservation of mass will imply that if all compounds containing a given species are captured by the model, the total mass of that species will be constant. This type of constraint will then give a conserved quantity of the form $c_i = H_i x$ where H_i represents that combinations of species in which the given element appears. Since c_i is constant, it follows that $\dot{c}_i = 0$ and, aggregating the set of all conserved species, we have

$$0 = \dot{c} = H\dot{x} = HNv(x,\theta) \quad \text{for all } x.$$

If we assume that the vector of fluxes spans $\mathbb{R}^m$ (the range of $v : \mathbb{R}^n \times \mathbb{R}^p \to \mathbb{R}^m$), then this implies that the conserved quantities correspond to the left null space of the stoichiometry matrix N.

   It is often useful to remove the conserved quantities from the description of the dynamics and write the dynamics for a set of independent species. To do this, we transform the state of the system into two sets of variables:

$$\begin{pmatrix} x_i \\ x_d \end{pmatrix} = \begin{pmatrix} P \\ H \end{pmatrix} x. \tag{3.15}$$

The vector $x_i = Px$ is the set of independent species and is typically chosen as a subset of the original species of the model (so that the rows P consists of all

zeros and a single 1 in the column corresponding to the selected species). The matrix H should span the left null space of N, so that x_d represents the set of dependent concentrations. These dependent species do not necessarily correspond to individual species, but instead are often combinations of species (for example, the total concentration of a given element that appears in a number of molecules that participate in the reaction).

Given the decomposition (3.15), we can rewrite the dynamics of the system in terms of the independent variables x_i. We start by noting that given x_i and x_d, we can reconstruct the full set of species x:

$$x = \begin{pmatrix} P \\ H \end{pmatrix}^{-1} \begin{pmatrix} x_i \\ x_d \end{pmatrix} = Lx_i + c_0, \qquad L = \begin{pmatrix} P \\ H \end{pmatrix}^{-1} \begin{pmatrix} I \\ 0 \end{pmatrix}, \qquad c_0 = \begin{pmatrix} P \\ H \end{pmatrix}^{-1} \begin{pmatrix} 0 \\ c \end{pmatrix}$$

where c_0 represents the conserved quantities. We now write the dynamics for x_i as

$$\dot{x}_i = P\dot{x} = PNv(Lx_i + c_0, \theta) = N_r v_r(x_i, c_0, \theta), \tag{3.16}$$

where N_r is the *reduced stoichiometry matrix* and v_r is the rate vector with the conserved quantities separated out as constant parameters.

The reduced order dynamics in equation (3.16) represent the evolution of the independent species in the reaction. Given x_i, we can "lift" the dynamics from the independent species to the full set of species by writing $x = Lx_i + c_0$. The vector c_0 represents the values of the conserved quantities, which must be specified in order to compute the values of the full set of species. In addition, since $x = Lx_i + c_0$, we have that
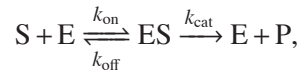
$$\dot{x} = L\dot{x}_i = LN_r v_r(x_i, c_0, p) = LN_r v(x, \theta),$$

which implies that

$$N = LN_r.$$

Thus, L also "lifts" the reduced stoichiometry matrix from the reduced space to the full space.

Example 3.4 (Enzyme kinetics). Consider an enzymatic reaction

$$S + E \underset{k_{off}}{\overset{k_{on}}{\rightleftharpoons}} ES \xrightarrow{k_{cat}} E + P,$$

whose full dynamics can be written as

$$\frac{d}{dt} \begin{pmatrix} S \\ E \\ ES \\ P \end{pmatrix} = \begin{pmatrix} -1 & 1 & 0 \\ -1 & 1 & 0 \\ 1 & -1 & -1 \\ 0 & 0 & 1 \end{pmatrix} \begin{pmatrix} k_{on} E \cdot S \\ k_{off} ES \\ k_{cat} ES \end{pmatrix}.$$

The conserved quantities are given by

$$H = \begin{pmatrix} 0 & 1 & 1 & 0 \\ 1 & -1 & 0 & 1 \end{pmatrix}.$$

The first of these is the total enzyme concentration $E_T = E + ES$, while the second asserts that the concentration of product P is equal to the free enzyme concentration E minus the substrate concentration S. If we assume that we start with substrate concentration S_0, enzyme concentration E_T and no product or bound enzyme, then the conserved quantities are given by

$$c = \begin{pmatrix} E + ES \\ S - E + P \end{pmatrix} = \begin{pmatrix} E_T \\ S_0 - E_T \end{pmatrix}.$$

There are many possible choices for the set of independent species $x_i = Px$, but since we are interested in the substrate and the product, we choose P as

$$P = \begin{pmatrix} 1 & 0 & 0 & 0 \\ 0 & 0 & 0 & 1 \end{pmatrix}.$$

Once P is chosen then we can compute

$$L = \begin{pmatrix} P \\ H \end{pmatrix}^{-1} \begin{pmatrix} I \\ 0 \end{pmatrix} = \begin{pmatrix} 1 & 0 \\ 1 & 1 \\ -1 & -1 \\ 0 & 1 \end{pmatrix}, \qquad c_0 = \begin{pmatrix} P \\ H \end{pmatrix}^{-1} \begin{pmatrix} 0 \\ c \end{pmatrix} = \begin{pmatrix} 0 \\ E_T - S_0 \\ S_0 \\ 0 \end{pmatrix},$$

The resulting reduced order dynamics can be computed to be

$$\frac{d}{dt} \begin{pmatrix} S \\ P \end{pmatrix} = \begin{pmatrix} -1 & 1 & 0 \\ 0 & 0 & 1 \end{pmatrix} \begin{pmatrix} k_{\mathrm{on}}(P + S + E_T - S_0)S \\ k_{\mathrm{off}}(-P - S + S_0) \\ k_{\mathrm{cat}}(-P - S + S_0) \end{pmatrix}$$

$$= \begin{pmatrix} -k_{\mathrm{on}}(P + S + E_T - S_0)S - k_{\mathrm{off}}(P + S - S_0) \\ k_{\mathrm{cat}}(S_0 - S - P) \end{pmatrix}.$$

A simulation of the dynamics is shown in Figure 3.10. We see that the dynamics are very well approximated as being a constant rate of production until we exhaust the substrate (consistent with the Michaelis-Menten approximation).

$$\nabla$$

Metabolic control analysis

Metabolic control analysis (MCA) focuses on the study of the sensitivity of steady state concentrations and fluxes to changes in various system parameters. The basic concepts are equivalent to the sensitivity analysis tools described in Section 3.2,
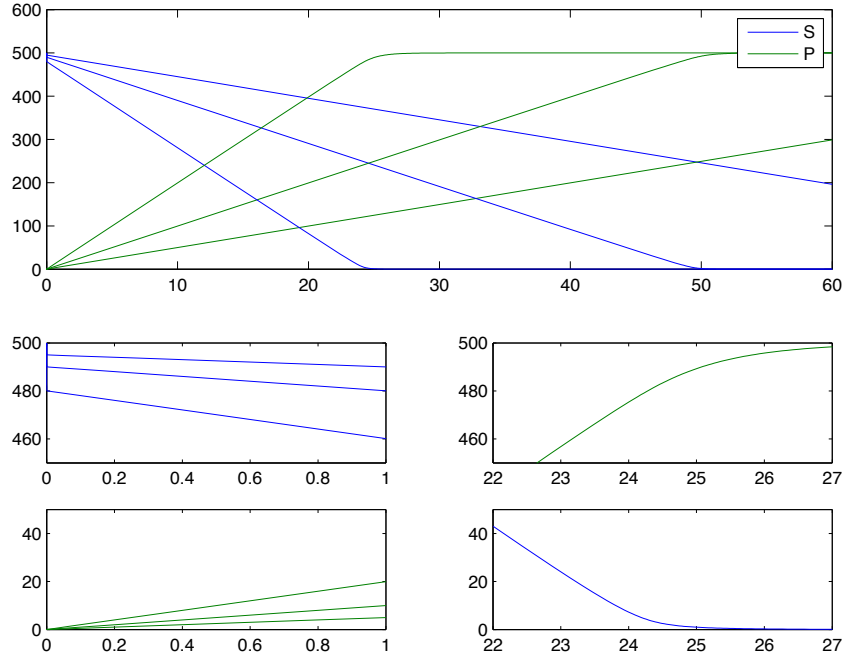
Figure 3.10: Enzyme dynamics. The simulations were carried out $k_{\mathrm{on}} = k_{\mathrm{off}} = 10$, $k_{\mathrm{cat}} = 1$, $S_0 = 500$ and $E_T = 5, 10 20$. The top plot shows the concentration of substrate S and product P, with the fastest case corresponding to $E_T = 20$. The figures on the lower left zoom in on the substrate and product concentrations at the initial time and the figures on the lower right at one of the transition times.

specialized to the case of reaction rate equations. In this section we provide a brief introduction to the key ideas, emphasizing the mapping between the general concepts and MCA terminology (as originally done by Ingalls [41]).

Consider the reduced set of chemical reactions

$$\dot{x}_i = N_r v_r(x_i, \theta) = N_r v(L x_i + c_0, \theta).$$

We wish to compute the sensitivity of the equilibrium concentrations x_e and equilibrium fluxes v_e to the parameters θ. We start by linearizing the dynamics around an equilibrium point x_e. Defining $z = x - x_e$, $u = \theta - \theta_0$ and $f(z, u) = N_r v(x_e + z, \theta_0 + u)$, we can write the linearized dynamics as

$$\dot{x} = Ax + Bu, \qquad A = \left(N_r \frac{\partial v}{\partial s} L \right), \quad B = \left(N_r \frac{\partial v}{\partial p} \right), \tag{3.17}$$

which has the form of a linear differential equation with state z and input u.

In metabolic control analysis, the following terms are defined:

$$\bar{\epsilon}_\theta = \frac{dv}{d\theta}\bigg|_{x_e,\theta_o} \qquad \bar{\epsilon}_\theta = \text{flux control coefficients}$$

$$\bar{R}_\theta^x = \qquad$$

$$\bar{R}_\theta^x = \frac{\partial x_e}{\partial \theta} = \bar{C}^x \bar{\epsilon}_\theta \qquad \bar{C}^x = \text{concentration control coefficients}$$

$$\bar{R}_\theta^v = \qquad$$

$$\bar{R}_\theta^v = \frac{\partial v_e}{\partial \theta} = \bar{C}^v \bar{\epsilon}_\theta \qquad \bar{C}^v = \text{rate control coefficients}$$

These relationships describe how the equilibrium concentration and equilibrium rates change as a function of the perturbations in the parameters. The two control matrices provide a mapping between the variation in the flux vector evaluated at equilibrium,

$$\left(\frac{\partial v}{\partial \theta}\right)_{x_e,\theta_0},$$

and the corresponding differential changes in the equilibrium point, $\partial x_e/\partial \theta$ and $\partial v_e/\partial \theta$. Note that

$$\frac{\partial v_e}{\partial \theta} \neq \left(\frac{\partial v}{\partial \theta}\right)_{x_e,\theta_0}.$$

The left side is the relative change in the equilibrium rates, while the right side is the change in the rate function $v(x,\theta)$ evaluated at an equilibrium point.

To derive the coefficient matrices $\bar{C}^x$ and $\bar{C}^v$, we simply take the linear equation (3.17) and choose outputs corresponding to s and v:

$$y_x = Ix, \qquad y_v = \frac{\partial v}{\partial x}Lx + \frac{\partial v}{\partial \theta}u.$$

Using these relationships, we can compute the transfer functions

$$H_x(s) = (sI - A)^{-1}B = \left[(sI - N_r\frac{\partial v}{\partial x}L)^{-1}N_r\right]\frac{\partial v}{\partial \theta},$$

$$H_v(s) = \frac{\partial v}{\partial s}L(sI - A)^{-1}B + \frac{\partial v}{\partial p} = \left[\frac{\partial v}{\partial x}L(sI - N_r\frac{\partial v}{\partial x}L)^{-1}N_r + I\right]\frac{\partial v}{\partial \theta}.$$

Classical metabolic control analysis considers only the equilibrium concentrations, and so these transfer functions would be evaluated at $x = 0$ to obtain the equilibrium equations.

These equations are often normalized by the equilibrium concentrations and parameter values, so that all quantities are expressed as fractional quantities. If we define

$$D^x = \text{diag}\{x_e\}, \qquad D^v = \text{diag}\{v(x_e, \theta_0)\}, \qquad D^\theta = \text{diag}\{\theta_0\},$$

the the normalized coefficient matrices (without the overbar) are given by

$$C^x = (D^x)^{-1}\bar{C}^x D^v, \qquad C^v = (D^v)^{-1}\bar{C}^v D^v,$$

$$R_\theta^x = (D^x)^{-1}\bar{R}_\theta^x D^\theta, \qquad R_\theta^v = (D^v)^{-1}\bar{R}_\theta^v D^\theta.$$

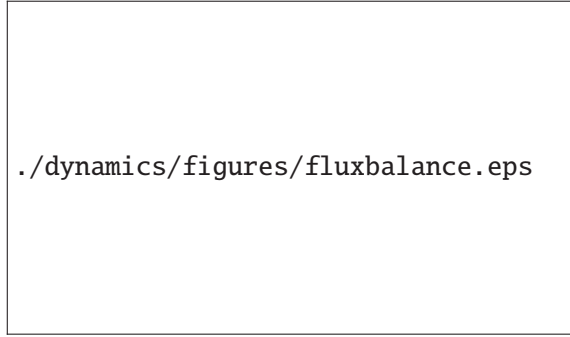**Example 3.5** (Enzyme kinetics)**.** TBA $\qquad\qquad \nabla$

Figure 3.11: Flux balance analysis.

Flux balance analysis

Flux balance analysis is a technique for studying the relative rate of different reactions in a complex reaction system. We are most interested in the case where there may be multiple pathways in a system, so that the number of reactions m is greater than the number of species n. The dynamics

$$\dot{x} = Nv(x, \theta)$$

thus have the property that the matrix N has more columns that rows and hence there are multiple reactions that can produce a given set of species. Flux balance is often applied to pathway analysis in metabolic systems to understand the limiting pathways for a given species and the the effects of changes in the network (e.g., through gene deletions) to the production capacity.

To perform a flux balance analysis, we begin by separating the reactions of the pathway into internal fluxes v_i versus exchanges flux v_e, as illustrated in Figure 3.11. The dynamics of the resulting system now be written as

$$\dot{x} = Nv(x, \theta) = N \begin{pmatrix} v_i \\ v_e \end{pmatrix} = Nv_i(x, \theta) - b_e,$$

where $b_e = -Nv_e$ represents the effects of external fluxes on the species dynamics. Since the matrix N has more columns that rows, it has a *right* null space and hence there are many different internal fluxes that can produce a given change in species.

In particular, we are interested studying the steady state properties of the system. In this case, we have that $\dot{x} = 0$ and we are left with an algebraic system

$$Nv_i = b_e.$$

Power law formalism

Chemical reaction rate equations are nonlinear differential equations whenever two or more species interact. However, the nonlinearities are very structured: they can be decomposed into a stoichiometry matrix and flux rates, and the flux rates typically consist of either polynomial terms or simple ratios of polynomials (e.g., Michaelis-Menten kinetics or Hill functions). In this section we consider power law representations that exploit these properties and attempt to provide simpler techniques for understand the relationships between species concentrations, parameter values and flux rates. This formalism was developed by Savageau [70] and is also called biochemical systems theory (BST).

The general power law formalism describes a set of reaction dynamics using a set of differential equations of the form

$$\frac{dx_i}{dt} = \sum_r E_r \prod_{j=1}^{n+m} x_j^{\epsilon_j^r} - \sum_s E_s \prod_{j=1}^{n+m} x_j^{\epsilon_j^s}, \quad i = 1, \ldots n. \tag{3.18}$$

Here, x_i is the concentration for species i, with $i = 1, \ldots, n$ representing internal species and $i = n + 1, \ldots, m$ representing external species, and the dynamics are broken into two summations. The first sum is over the set of reactions that produce the species x_i and the second is over the reactions that utilize x_i (and so decrease its concentration). The linear coefficients E_r and E_s are the activity levels and correspond to the rate constants (for metabolic networks the rate constants are often proportional to a fixed enzyme level, hence the use of the symbol E). The exponents ϵ_j^r and ϵ_i^s are the *kinetic orders* of the production and utilization reactions.

In this general form, the power law formalism is able to exactly capture mass action kinetics, but it does not provide any additional structure. If we consider a general rate equation of the form $v_i(x_1, \ldots, x_{n+m})$, we can approximate this function in a number of ways. The first is through its linearization,

$$v_i(x_1, \ldots, x_{n+m}) \approx v_i(x_{1,e}, \ldots, x_{n+m,e}) + \sum \frac{\partial v}{\partial x_j}(x_j - x_{j,e}) + \text{higher order terms.}$$

We have used exactly this approximation in previous sections.

A different approximation can be obtained by taking a Taylor series expansion for $\log v_i$:

$$\log v_i(x_1, \ldots, x_{n+m}) \approx \log v_i(x_{1,e}, \ldots, x_{n+m,e}) + \sum \frac{\partial \log v_i}{\partial \log x_j}(\log x_i - \log x_{i,e}) + \text{higher order terms.}$$

If we define

$$g_{i,j} = \frac{\partial \log v_i}{\partial \log x_j} = \frac{x_j}{v_i} \cdot \frac{\partial v_i}{\partial x_j}$$

and collect terms, we have

$$\log v_i(x) \approx \log \alpha_i + g_{i,1} \log x_1 + \cdots + g_{i,n+m} \log x_{n+m}.$$

Converting this back from log coordinates, we can thus right

$$v_i(x) \approx \alpha_i \prod_{j=1}^{n+m} x_j^{g_{i,j}}.$$

Using this approximation on the sums in equation (3.18), we can approximate the resulting dynamics as

$$\frac{dx_i}{dt} = \alpha_i \prod x_j^{g_{i,j}} - \beta_i \prod x_j^{h_{i,j}},$$

where α_i and $g_{i,j}$ are the rate constant and kinetic orders for the production terms and β_i and $h_{i,j}$ are the rate constant and kineeetic orders for reactions that utilize x_i. While this is only an approximation, its form is convenientt for performing equilibrium analyses. In particular, if $\dot{x}_i = 0$ then we can equate the production rate to the utilization rate adn take the log of this expression to obtain

$$\log \alpha_i + \sum g_{i,j} \log x_j = \log \beta_i + \sum h_{i,j} \log x_j.$$

This is now a linear equation for the logs of the concentrations in terms of the various parameters that enter the system.

3.5   Oscillatory Behavior

In addition to equilibrium behavior and input/output transfer curves, a variety of cellular procesess involve oscillatory behavior in which the system state is constantly changing, but in a repeating pattern. Two examples of biological oscillations are the cell cycle and circadian rhythm. Both of these dynamic behaviors involve repeating changes in the concentrations of various proteins, complexes and other molecular species in the cell, though they are very different in their operation. In this section we discuss some of the underlying ideas for how to model this type of oscillatory behavior, focusing on those types of oscillations that are most common in biomolecular systems.

Biomolecular oscillators

Biological systems have a number of natural oscillatory processes that govern the behavior of subsystems and whole organisms. These range from internal oscillations within cells to the oscillatory nature of the beating heart to various tremors and other undesirable oscillations in the neuro-muscular system. At the biomolecular level, two of the most studied classes of oscillations are the cell cycle and circadian rhythm.

The cell cycle consists of a set "phases" that govern the duplication and division of cells into two new cells:

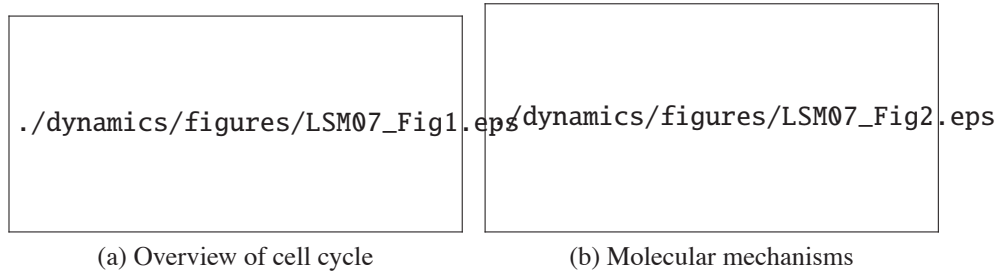(a) Overview of cell cycle   (b) Molecular mechanisms

Figure 3.12: The *Caulobacter crescentus* cell cycle. (a) *Caulobacter* cells divide asymmetrically into a stalked cell, which is attached to a surface, and a swarmmer cell, that is motile. The swarmer cells can become stalked cells in a new location and begin the cell cycle anew. The transcriptional regulators CtrA, DnaA and GcrA are the primary factors that control the various phases of the cell cycle. (b) The genetic circuitry controlling the cell cycle consists of a large variety of regulatory mechanisms, described in more detail in the text. Figure obtained from [48] (permission TBD).

- G1 phase - gap phase, terminated by "G1 checkpoint"

- S phase - synthesis phase (DNA replication)

- G2 phase - gap phase, terminated by "G2 checkpoint"

- M - mitosis (cell division)

The cell goes through these stages in a cyclical fashion, with the different enzymes and pathways active in different phases. The cell cycle is regulated by many different proteins, often divided into two major classes. *Cyclinscyclins* are a class of proteins that sense environmental conditions internal and external to the cell and are also used to implement various logical operations that control transition out of the G1 and G2 phases. *Cyclin dependent kinases* (CDKs)are proteins that serve as "actuators" by turning on various pathways during different cell cycles.

An example of the control circuitry of the cell cycle for the bacterium *Caulobacter crescentus* (henceforth *Caulobacter*) is shown in Figure 3.12 [48]. This organism uses a variety of different biomolecular mechanisms, including transcriptional activation and represssion, positive autoregulation (CtrA), phosphotransfer and methlylation of DNA.

The cell cycle is an example of an oscillator that does not have a fixed period. Instead, the length of the individual phases and the transitioning of the different phases are determined by the environmental conditions. As one example, the cell division time for *E. coli* can vary between 20 minutes and 90 minutes due to changes in nutrient concentrations, temperature or other external factors.

A different type of oscillation is the highly regular pattern encoding in circadian rhythm, which repeat with a period of roughly 24 hours. The observation of circadian rhythms dates as far back as 400 BCE, when Androsthenes described

./dynamics/figures/BP+05_Fig1.eps

Figure 3.13: *Caption omitted pending permission*. (Figure and caption from [13])

observations of daily leaf movements of the tamirind tree [52]. There are three defining characteristics associated with circadian rhythm: (1) the time to complete one cycle is approximately 24 hours, (2) the rhythm is endogenously generated and self-sustaning and (3) the period remains relatively constant under changes in ambient temperature. Oscillations that have these properties appaer in many different organisms, including micro-organisms, plants, insects and mammals. Some common features of the circuitry implementing circadian rhythms in these organisms is the combination of postive and negative feedback loops, often with the positive elements activating the expression of clock genes and the negative elements repressing the positive elements [13]. Figure 3.13 shows some of the different organisms in which circadian oscillations can be found and the primary genes responsible for different postive and negative factors.

Clocks, oscillators and limit cycles

To begin our study of oscillators, we consider a nonlinear model of the system described by the differential equation

$$\frac{dx}{dt} = f(x, u, \theta), \qquad y = h(x, \theta)$$

where $x \in \mathbb{R}^n$ represents the state of the system (typically concentrations of various proteins and other species and complexes), $u \in \mathbb{R}^q$ represents the external inputs, $y \in$

$\mathbb{R}^p$ represents the (measured) outputs and $\theta \in \mathbb{R}^K$ represents the model parameters. We say that a solution $(x(t), u(t))$ is *oscillatory with period T* if $y(t+T) = y(t)$. For simplicity, we will often assume that $p = q = 1$, so that we have a single input and single output, but most of the results can be generalized to the multi-input, multi-output case.

There are multiple ways in which a solution can be oscillatory. One of the simplest is that the input $u(t)$ is oscillatory, in which case we say that we have a *forced oscillation*. In the case of a linear system, an input of the form $u(t) = A \sin \omega t$ then we now already the output will be of the form $y(t) = M \cdot A \sin(\omega t + \phi)$ where M and ϕ represent the gain and phase of the system (at frequency ω). In the case of a nonlinear system, if the output is periodic then we can write it in terms of a set of harmonics,

$$y(t) = B_0 + B_1 \sin(\omega t + \phi_1) + B_2 \sin(2\omega t + \phi_2) + \cdots$$

The term B_0 represents the average value of the output (also called the bias), the terms B_i are the magnitudes of the ith harmonic and ϕ_i are the phases of the harmonics (relative to the input). The *oscillation frequency* ω is given by $\omega = 2\pi/T$ where T is the oscillation period.

A different situation occurs when we have no input (or a constant input) and still obtain an oscillatory output. In this case we say that the system has a *self-sustained oscillation*. This type of behavior is what is required for oscillations such as the cell cycle and circadian rhythm, where there is either no obvious forcing function or the forcing function is removed by the oscillation persists. If we assume that the input is constant, $u(t) = A_0$, then we are particularly interested in how the period T (or equivalently frequency ω), amplitudes B_i and phases ϕ_i depend on the input A_0 and system parameters θ.

To simplify our notation slightly, we consider a system of the form

$$\frac{dx}{dt} = F(x, \theta), \qquad y = h(x, \theta) \tag{3.19}$$

where $F(x, \theta) = f(x, u, \theta)$ reflects the fact that the input is ignored (or taken to be one of the constant parameters) in the analysis that follows. We have focused on the oscillatory nature of the output $y(t)$ thus far, but we note that if the states $x(t)$ are periodic then the output is as well, as this is the most common case. Hence we will often talk about the *system* being oscillatory, by which we mean that there is a solution for the dynamics in which the state satisfies $x(t+T) = x(t)$.

More formally, we say that a closed curve $\Gamma \in \mathbb{R}^n$ is an *orbit* if trajectories that start on Γ remain on Γ for all time and if Γ is not an equilibrium point of the system. As in the case of equilibrium points, we say that the orbit is *stable* if trajectories that start near Γ stay near Γ, *asymptotically stable* if in addition nearby trajectories approach Γ as $t \to \infty$ and *unstable* if it is not stable. The orbit Γ is periodic with period T if for any $x(t) \in \Gamma$, $x(t+T) = x(t)$.

(a) Linear harmonic oscillator   (b) Nonlinear harmonic oscillator
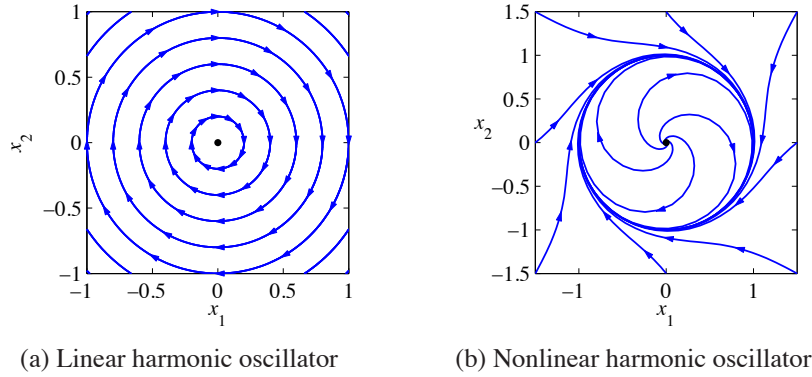
Figure 3.14: Examples of harmonic oscillators.

.

There are many different types of periodic orbits that can occur in a system whose dynamics are modeled as in equation (3.19). A *harmonic oscillator* references to a system that oscillates around an equilibrium point, but does not (usually) get near the equilibrium point. The classical harmonic oscillator is a linear system of the form

$$\frac{d}{dt} \begin{pmatrix} 0 & \omega \\ -\omega & 0 \end{pmatrix} \begin{pmatrix} x_1 \\ x_2 \end{pmatrix},$$

whose solutions are given by

$$\begin{pmatrix} x_1(t) \\ x_2(t) \end{pmatrix} = \begin{pmatrix} \cos\omega t & \sin\omega t \\ -\sin\omega t & \cos\omega t \end{pmatrix} \begin{pmatrix} x_1(0) \\ x_2(0) \end{pmatrix}.$$

The frequency of this oscillation is fixed, but the amplitude depends on the values of the initial conditions, as shown in Figure 3.14. Note that this system has a single equilibrium point at $x = (0,0)$ and the eigenvalues of the equilibrium point have zero real part, so trajectories neither expand nor contract, but simply oscillate.

An example of a nonlinear harmonic oscillator is given by the equation

$$\frac{dx_1}{dt} = x_2 + x_1(1 - x_1^2 - x_2^2), \qquad \frac{dx_2}{dt} = -x_1 + x_2(1 - x_1^2 - x_2^2). \tag{3.20}$$

This system has an equilibrium point at $x = (0,0)$, but the linearization of this equilibrium point can be shown to be unstable. The phase portrait in Figure **??** shows that the solutions in the phase plane converge to a circular trajectory. In the time domain this corresponds to an oscillatory solution. Mathematically the circle is called a *limit cycle*. Note that in this case, the solution for any initial condition approaches the limit cycle and the amplitude and frequency of oscillation "in steady state" (once we have reached the limit cycle) are independent of the initial condition.
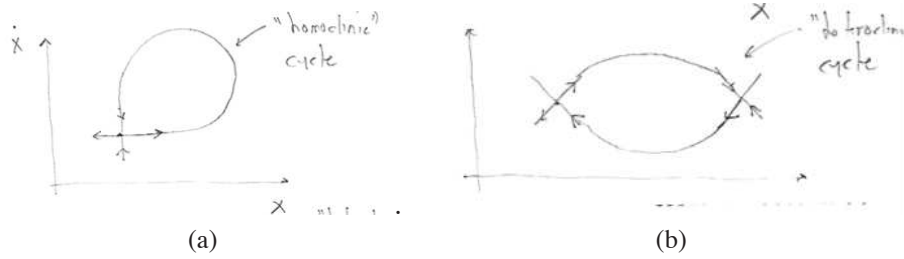
Figure 3.15: Homoclinic and heteroclinic orbits

.

A different type of oscillation can occur in nonlinear systems in which the equlibrium points are saddle points, having both stable and unstable eigenvalues. Of particular interest is the case where the stable and unstable orbits of one or more equilibrium points join together. Two such sitautions are shown in Figure 3.15. The figure on the left is an example of a *homoclinic orbit*. In this system, trajectories that start near the equilibrium point quickly diverge away (in the directions corresponding to the unstable eigenvalues) and then slowly return to the equilibrium point along the stable directions. If the initial conditions are chosen to be precisely on the homoclinic orbit Γ then the system slowly converges to the equilibrium point, but in practice there are often disturbances present that will perturb the system off of the orbit and trigger a "burst" in which the system rapidly escapes from the equilibrium point and then slowly converges again.

A somewhat similar type of orbit is a *heteroclinic orbit*, in which the orbit connects two different equilibrium points, as shown in Figure 3.15b.

An example of a system with a homoclinic orbit is given by the system

$$\frac{dx_1}{dt} = x_2, \qquad \frac{dx_2}{dt} = x_1 - x_1^3 \qquad (3.21)$$

The phase portrait and time domain solutions are shown in Figure 3.16. In this system, there are periodic orbits both inside and outside the two homoclinic cycles (left and right). Note that the trajectory we have chosen to plot in the time domain has the property that it rapidly moves away from the equilibrium point and then slowly re-converges to the equilibrium point, before begin carried away again. This type of oscillation, in which one slowly returns to an equilibrium point before rapidly diverging is often called a *relaxation oscillation*. Note that for this system, there are also oscillations that look more like the harmonic oscillator case described above, in which we oscillate around the unstable equilibirum points at $x = (\pm 1, 0)$.
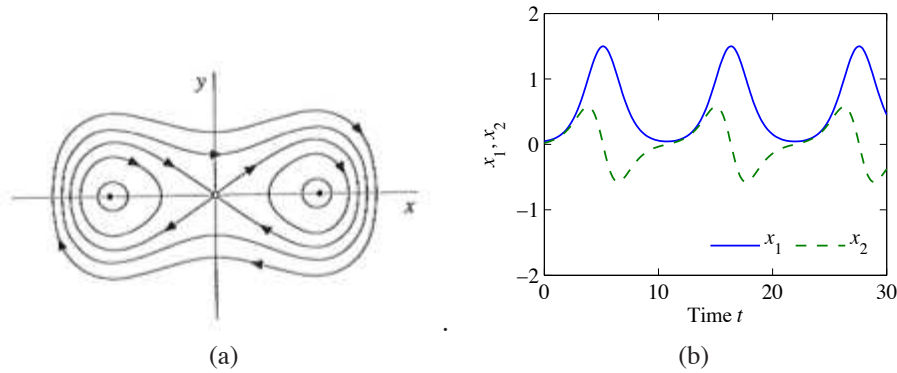
(a)   (b)

Figure 3.16: Example of a homoclinic orbit.

Limit cycles in the plane

Before studying periodic behavior of systems in $\mathbb{R}^n$, we study the behavior of systems in $\mathbb{R}^2$ as several high dimensional systems can be often well approximated by systems in two dimensions by, for example, employing quasi-steady state approximations. For systems in $\mathbb{R}^2$, we will see that there are only two types of solutions: those converging (diverging) from steady states and periodic solutions. That is, chaos can be ruled out in two-dimensional systems.

Consider the system $\dot{x} = F(x)$, in which $F(x)$ is often referred to as vector field, and let $x(t, x_0)$ denote its solution starting at x_0 at time $t = 0$, that is, $\dot{x}(t, x_0) = F(x(t, x_0))$ and $x(0, x_0) = x_0$. We say that $x(t, x_0)$ is a *periodic solution* if there is $T > 0$ such that $x(t, x_0) = x(t + T, x_0)$ for all $t \in \mathbb{R}$. Here, we seek to answer two questions: (a) when does a system $\dot{x} = F(x)$ admit periodic solutions? (b) When are these periodic solutions stable or asymptotically stable?

We first tackle these questions for the case $x \in \mathbb{R}^2$. The first result that we next give provides a simple check to rule out periodic solutions for system in $\mathbb{R}^2$. Specifically, let $x \in \mathbb{R}^2$ and consider

$$\dot{x}_1 = F_1(x_1, x_2) \qquad \dot{x}_2 = F_2(x_1, x_2), \qquad (3.22)$$

in which the functions $F : \mathbb{R}^2 \to \mathbb{R}^2$ is smooth. Then, we have the following result:

Theorem 3.2 (Bendixson's Criterion)**.** *If on a simply connected region $D \subset \mathbb{R}^2$ (i.e., there are no holes in it) the expression*

$$\frac{\partial F_1}{\partial x_1} + \frac{\partial G_2}{\partial x_2}$$

is not identically zero and does not change sign, then system (3.22) has no closed orbits that lie entirely in D.

Example 3.6. Consider the system

$$\dot{x}_1 = -x_2^3 + \delta x_1^3, \qquad \dot{x}_2 = x_1^3,$$

with $\delta \geq 0$. We can compute $\frac{\partial F_1}{\partial x_1} + \frac{\partial F_2}{\partial x_2} = 3\delta x_1^2$, which is positive in all $\mathbb{R}^2$ if $\delta \neq 0$. If $\delta \neq 0$, we can thus conclude from Bendixson's criterion that there are no periodic solutions. Investigate as an exercise what happens when $\delta = 0$. $\qquad \nabla$

In order to provide the main result to state the existence of a stable periodic solution, we need the concept of omega-limit set of a point p, denoted $\omega(p)$. Basically, the omega-limit set $\omega(p)$ denotes the set of all points to which the trajectory of the system starting from p tends as time approaches infinity. This is formally defined in the following definition.

Definition 3.1. A point $\bar{x} \in \mathbb{R}^n$ is called an *omega-limit point* of $p \in \mathbb{R}^n$ if there is a sequence of times $\{t_i\}$ with $t_i \to \infty$ for $i \to \infty$ such that $x(t_i, p) \to \bar{x}$ as $i \to \infty$. The *omega limit set* of p, denoted $\omega(p)$, is the set of all omega-limit points of p.

The omega-limit set of a system has several relevant properties, among which the fact that it cannot be empty and that it must be a connected set.

The following theorem, completely characterizes the omega limit set of any point for a system in $\mathbb{R}^2$.

Theorem 3.3 (Poincarè-Bendixson). *Let M be a positively invariant region for the system $\dot{x} = F(x)$ with $x \in \mathbb{R}^2$ (i.e., any trajectory that starts in M stays in M for all $t \geq 0$). Let $p \in M$, then one of the following possibilities holds for $\omega(p)$:*

 (i) $\omega(p)$ *is a steady state;*

 (ii) $\omega(p)$ *is a closed orbit;*

 (iii) $\omega(p)$ *consists of a finite number of steady states and orbits, each starting (for $t = 0$) and ending (for $t \to \infty$) at one of the fixed points.*

This theorem has two important consequences:

1. If the system does not have steady states in M, since $\omega(p)$ is not empty, it must be a periodic solution;

2. If there is only one steady state in M and it is unstable and not a saddle (i.e., the eigenvalues of the linearization at the steady state are both positive), then $\omega(p)$ is a periodic solution.

Example 3.7. Consider the following system in $\mathbb{R}^2$:

$$\dot{x}_1 = x_1 - x_2 - (x_1^2 + x_2^2)x_1, \qquad \dot{x}_2 = x_1 + x_2 - (x_1^2 + x_2^2)x_2.$$

Verify as an exercise that this system admits one equilibrium point only (the origin), which is unstable. Also, show that its trajectories are globally bounded (for example, take a set $x_1^2 + x_2^2 = c$ for c large enough and demonstrate that the vector field of the system always points inside the circle $x_1^2 + x_2^2 = c$). Therefore, by Poincarè-Bendixson Theorem, we can conclude that the omega-limit set of any point in $\mathbb{R}^2$ different from the origin is a non-zero periodic orbit.　　　　　∇

Limit cycles in $\mathbb{R}^n$

The results above holds only for systems in two dimensions. However, there have been recent extensions of this theorem to systems with special structure in $\mathbb{R}^n$. In particular, we have the following result due to Hastings et al. (1977).

Theorem 3.4 (Hastings et al. 1977)**.** *Consider a system $\dot{x} = F(x)$, which is of the form*

$$\dot{x}_1 = F_1(x_n, x_1)$$
$$\dot{x}_j = F_j(x_{j-1}, x_j),\ 2 \le j \le n$$

on the set M defined by $x_i \ge 0$ for all i with the following inequalities holding in M:

(i) *$\frac{\partial F_i}{\partial x_i} < 0$ and $\frac{\partial F_i}{\partial x_{i-1}} > 0$, for $2 \le i \le n$, and $\frac{\partial F_1}{\partial x_n} < 0$;*

(ii) *$F_i(0,0) \ge 0$ and $F_1(x_n, 0) > 0$ for all $x_n \ge 0$;*

(iii) *The system has a unique steady state $x^* = (x_1^*, ..., x_n^*)$ in M such that $F_1(x_n, x_1) < 0$ if $x_n > x_n^*$ and $x_1 > x_1^*$, while $F_1(x_n, x_1) > 0$ if $x_n < x_n^*$ and $x_1 < x_1^*$;*

(iv) *$\frac{\partial F_1}{\partial x_1}$ is bounded above in M.*

Then, if the Jacobian of f at x^* has no repeated eigenvalues and has any eigenvalue with positive real part, then the system has a non-constant periodic solution in M.

　　This theorem states that for a system with cyclic structure in which the cycle "has negative gain", the instability of the steady state (under some technical assumption) is equivalent to the existence of a periodic solution. This'theorem, however, does not provide information about whether the orbit is attractive or not, that is, of whether it is an omega-limit set of any point in M. This stability result is implied by a more recent theorem due to Mallet-Paret and Smith (1990), for which we provide a simplified statement as follows.

Theorem 3.5 (Mallet-Paret and Smith, 1990)**.** *Consider the system $\dot{x} = F(x)$ with the following cyclic feedback structure*

$$\dot{x}_1 = F_1(x_n, x_1)$$
$$\dot{x}_j = F_j(x_{j-1}, x_j),\quad 2 \le j \le n$$

on a set M defined by $x_i \geq 0$ for all i with all trajectories starting in M bounded for $t \geq 0$. Then, the omega-limit set $\omega(p)$ of any point $p \in M$ can be one of the following:

(a) A steady state;

(b) A non-constant periodic orbit;

(c) A set of steady states connected by homoclinic or heteroclinic orbits.

A heteroclinic orbit is an orbit that starts (for $t = 0$) at a steady state and ends (for $t \to \infty$) into a different steady state. A homoclinic orbit is an orbit that starts and ends at the same steady state. It is thus clear that a steady state whose linearization has eigenvalues with all positive or all negative real parts cannot have a homoclinic orbit. As a consequence of the theorem, then we have that for a system with cyclic feedback structure that admits one steady state only and at which the linearization has all eigenvalues with positive real part, the omega limit set must be a periodic orbit.

Let for some $\delta_i \in \{1, -1\}$ be $\delta_i \frac{\partial F_i(x, x_{i-1})}{\partial x_{i-1}} > 0$ for all $0 \leq i \leq n$ and define $\Delta := \delta_1 \cdot ... \cdot \delta_n$. One can show that the sign of Δ is related to whether the system has one or multiple steady states.

Therefore, a system with a cyclic feedback structure and a unique equilibrium point at which the linearization has all eigenvalues with positive real part admits a stable periodic orbit.

3.6 Analysis Using Describing Functions

Unlike the case of linear systems, where it is possible to full characterize the solutions of a model and there are a wide variety of analysis techniques available, the behavior of nonlinear systems is harder to analyze, especially away from equilibrium points (where the linearization gives a good approximation). One of the more useful techniques for studying the behavior of nonlinear systems is the method of harmonic balance, of which a special case is the method of describing functions. This section explores the use of harmonic balance and describing functions for analyzing nonlinear systems, including the detection and analysis of limit cycles and the propagation of noise through nonlinear systems.

Describing functions (AM08)

For special nonlinear systems like the one shown in Figure 3.17a, which consists of a feedback connection between a linear system and a static nonlinearity, it is possible to obtain a generalization of Nyquist's stability criterion based on the idea of *describing functions*. Following the approach of the Nyquist stability condition,
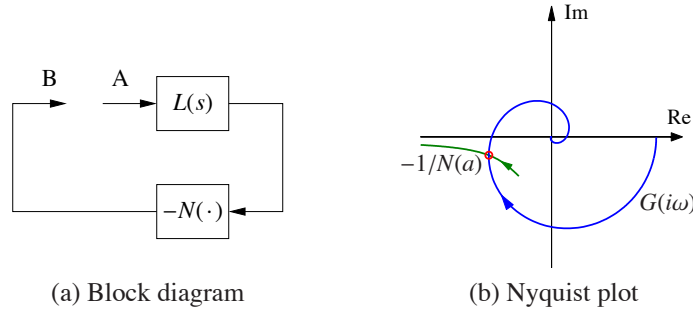
(a) Block diagram   (b) Nyquist plot

Figure 3.17: Describing function analysis. A feedback connection between a static nonlin-earity and a linear system is shown in (a). The linear system is characterized by its transfer function $L(s)$, which depends on frequency, and the nonlinearity by its describing function $N(a)$, which depends on the amplitude a of its input. The Nyquist plot of $L(i\omega)$ and the plot of the $-1/N(a)$ are shown in (b). The intersection of the curves represents a possible limit cycle.

we will investigate the conditions for maintaining an oscillation in the system. If the linear subsystem has low-pass character, its output is approximately sinusoidal even if its input is highly irregular. The condition for oscillation can then be found by exploring the propagation of a sinusoid that corresponds to the first harmonic.

To carry out this analysis, we have to analyze how a sinusoidal signal propagates through a static nonlinear system. In particular we investigate how the first harmonic of the output of the nonlinearity is related to its (sinusoidal) input. Letting F represent the nonlinear function, we expand $F(e^{i\omega t})$ in terms of its harmonics:

$$F(ae^{i\omega t}) = \sum_{n=0}^{\infty} M_n(a)e^{i(n\omega t + \phi_n(a))},$$

where $M_n(a)$ and $\phi_n(a)$ represent the gain and phase of the nth harmonic, which depend on the input amplitude since the function F is nonlinear. We define the describing function to be the complex gain of the first harmonic:

$$N(a) = M_1(a)e^{i\phi_n(a)}. \tag{3.23}$$

The function can also be computed by assuming that the input is a sinusoid and using the first term in the Fourier series of the resulting output.

Arguing as we did when deriving Nyquist's stability criterion, we find that an oscillation can be maintained if

$$L(i\omega)N(a) = -1. \tag{3.24}$$

This equation means that if we inject a sinusoid at A in Figure 3.17, the same signal will appear at B and an oscillation can be maintained by connecting the
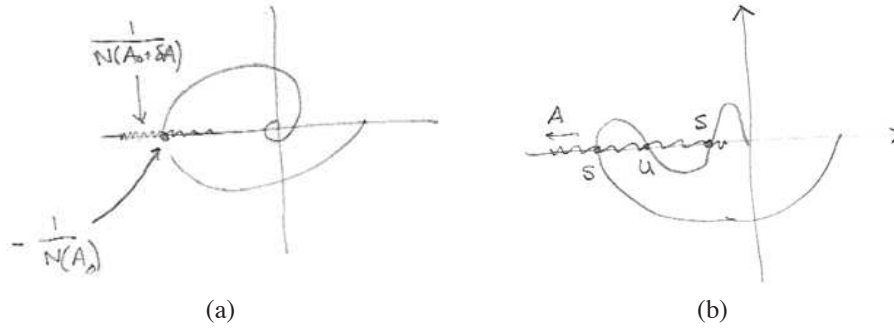
(a)   (b)

Figure 3.18: Heuristic stability of limit cycles using describing functions. (a) To check if a perturbation from amplitude a_0 to amplitude $a_0 + \delta a$ is stabilizing, we check to see if the Nyquist criterion is satisfied for the original frequency response and the perturbed critical point $P_1 = 1/N(a_0 + \delta a)$. (b) An example of a nonlinear system with multiple limit cycles. Stable limit cycles are labeled 's' and unstable limit cycles are labeled 'u'.

points. Equation (3.24) gives two conditions for finding the frequency ω of the oscillation and its amplitude a: the phase must be $180°$, and the magnitude must be unity. A convenient way to solve the equation is to plot $L(i\omega)$ and $-1/N(a)$ on the same diagram as shown in Figure 3.17b. The diagram is similar to the Nyquist plot where the critical point -1 is replaced by the curve $-1/N(a)$ and a ranges from 0 to ∞.

It is possible to define describing functions for types of inputs other than sinusoids. Describing function analysis is a simple method, but it is approximate because it assumes that higher harmonics can be neglected. Excellent treatments of describing function techniques can be found in the texts by Atherton [6] and Graham and McRuer [32].

Example 3.8 (Repressilator).   ▽

Stability of limit cycles using describing functions

In order to check the stability of a limit cycle, we must reason about how solutions that have initial conditions near the limit cycle evolve in time and whether they move closer to the limit cycle (asymptotic stability) or diverge from the limit cycle (instability).

We begin by arguing heuristically, using the Nyquist plot in Figure 3.17b. Suppose that we were to consider a perturbed limit cycle with amplitude $a_0 + \delta a$, where a_0 is the amplitude of the limit cycle predicted by the describing function method. If we did so, then the point of intersection of the describing function and the frequency response would move from $P_0 = -1/N(a_0)$ to $P_1 = -1/N(a_0 + \delta a)$, as shown in Figure 3.18a. Now evaluate the Nyquist criterion for the frequency response with

critical point P_1. If the criterion indicates that the perturbed system is stable (i.e., no net encirclements of P_1 for a stable process), then intuitively the amplitude of the perturbed solution would decrease and we would return to our original amplitude limit cycle. Conversely, if the Nyquist criterion with critical point P_1 indicates instability, then the oscillation would grow and hence we can infer that the limit cycle is unstable. Figure 3.18b shows a situation with multiple limit cycles with some stable and some unstable.

While this heuristic method is intuitively appealing, it does not always give the correct answer. Indeed, even the prediction of the existence of a limit cycle using describing functions can be incorrect unless the system satisfies some additional conditions. We present here one such set of conditions, due to Mees [**?**].

Suppose that (ω_0, a_0) satisfies the describing function balance equation $P(i\omega_0) = -1/N(a_0)$ and that the the frequency response curve and the describing function locus are transverse (not tangent) at their intersection. Define

$$\rho(\omega)^2 = \sum_{k=3,5,9,\dots} |P(ik\omega_0)|^2, \qquad \text{``gain of harmonics''}$$

$$p(a)^2 = \|n(a\sin t)\|_2^2 - |aN(a)|^2, \qquad \text{``first harmonic error''}$$

$$q(a,\epsilon) = \|m(a\sin t, \epsilon)\|_2, \qquad \text{``slope bound''}$$

$$m(x,\epsilon) = \max\{|N(x+\epsilon) - N(x)|, |N(x-\epsilon) - N(x)|\}.$$

Now find an ϵ such that for all (ω, a) near (ω, a_0),

$$\rho(\omega)(p(a) + q(a,\epsilon)) \le \epsilon$$

and let $\Omega \in \mathbb{R}_+^2$ be the set of (ω, a) such that

$$|N(a) + 1/G(i\omega)| \le q(a,\epsilon)/a.$$

Theorem 3.6. *Suppose Ω is bounded and there exists a unique $(\omega, a_0) \in \Omega$ satisfying the balance equation. Then there exists a periodic solution of the form $y(t) = a\sin(\omega t) + y^*(t)$ with remnant $\|y^*\|_\infty \le \epsilon$.*

Sketch of proof. Reduced to the contraction mapping theorem, which generates ρ, p and q.   □

The basic idea behind this theorem is that if the harmonics around the loop decay sufficiently quickly (determined by the frequency response), then we can insure that there is truly a periodic solution and bound the error of the higher harmonics. There is also a graphical version of the stability theorem that checks for "complete intersections" between the describing function locus and the Nyquist curve [**?**].

Mathematically, the stability of a limit cycle can be analyzed by taking the lin-
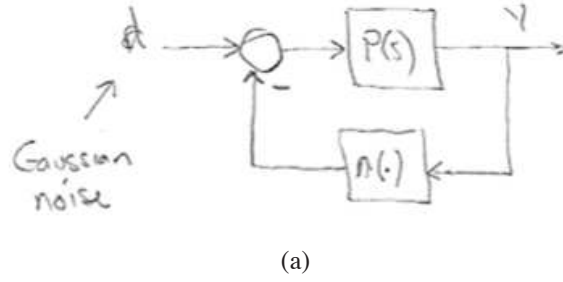
(a)

Figure 3.19: Random input describing function analysis.

earization of the system around the (non-equilibrium) solution. To see how this is done, consider a nonlinear system of the form

$$\dot{x} = f(x)$$

that has a solution $x_d(t)$ that is periodic with period T. To compute the linearization of the dynamics around the equilibrium point, we compute the dynamics of the error $e = x - x_d$:

$$\dot{e} = f(x) - f(x_d) = F(e, x_d(t)) \approx A(t)e$$

where $A(t)$ is the time-varying linearization given by

$$A(t) = \left. \frac{\partial F}{\partial e}(e, x_d) \right|_{e=0, x_d(t)}.$$

The dynamics matrix $A(t)$ is periodic and so the dynamics of the linearization are a given by a periodic, linear ordinary differential equation.

The dynamics of periodic linear systems can be studied using *Floquet* theory, which we briefly review here. Let $\Phi(t,0)$ be the (T-periodic) fundamental matrix for $\dot{e} = A(t)e$, so that the solution is given by $x(t) = \Phi(t,0)x(0)$. It can be show that $\Phi(t,0)$ has the form $\phi(t,0) = P(t)e^{Ft}$ where $P(t) = P(t+T) \in \mathbb{R}^{n \times n}$ is a periodic matrix and $F \in \mathbb{R}^{n \times n}$ is a constant matrix. We can now check stability by examining the eigenvalues of the matrix e^{FT}, which corresponds to the "first return" map for the system.

Random input describing functions

In addition to allowing prediction and analysis of limit cycles, describing functions can also be used to analyze the propagation of noise through nonlinear feedback systems. This approach is known as the *random input describing function* method.

As in the single input describing function method, we begin with a system in the form of a linear system with a nonlinear feedback, as shown in Figure 3.19a. To analyze this system, we construct an input that contains both a sinusoid and a

random input $r(t)$:

$$y = b + a\sin(\omega t + \phi) + r(t),$$

where b is the bias term, a is the amplitude of the sinusoidal term, ϕ is a uniform random variable and $r(t)$ is a stationary Gaussian random process with variance σ^2 and correlation $\rho(\tau)$.[1] We approximate the response of the system through the nonlinearity by

$$N(y(t)) \approx N_b b + N_a a\sin(\omega t + \phi) + N_r r(t),$$

where N_b is called the *bias gain*, N_a is the sinusoidal gain and N_r is the stochastic gain. These functions are given by

$$N_b(b,a,\sigma) = \frac{1}{b}E\{f(y)\} = \frac{1}{(2\pi)^{3/2}\sigma b} \int_0^{2\pi} \int_{-\infty}^{\infty} f(b + a\sin\theta + r(t))e^{-\frac{r^2}{2\sigma^2}} \, dr \, d\theta$$

$$N_a(b,a,\sigma) = \frac{2}{a}E\{f(y)\sin\theta\} = \frac{2}{(2\pi)^{3/2}\sigma a} \int_0^{2\pi} \int_{-\infty}^{\infty} f(b + a\sin\theta + r(t))\sin\theta \, e^{-\frac{r^2}{2\sigma^2}} \, dr \, d\theta$$

$$N_r(b,a,\sigma) = \frac{1}{\sigma^2}E\{f(y)r\} = \frac{1}{(2\pi)^{3/2}\sigma^3} \int_0^{2\pi} \int_{-\infty}^{\infty} f(b + a\sin\theta + r(t))r \, e^{-\frac{r^2}{2\sigma^2}} \, dr \, d\theta$$

$$\tag{3.25}$$

The random input describing function method has a number of special cases. If we take $\sigma = 0$, then it can be shown that we recover the standard describing function method. If we instead take $a = 0$, we can study how noise propagates through the system. Recall that in the linear case, where the feedback term is given by a constant gain N, the spectral density of the output y is given by

$$S_y(\omega) = H_{yd}(-i\omega)S_d(\omega)H_{yd}(i\omega), \qquad \sigma_y = \frac{1}{2\pi}\int_{-\infty}^{\infty} S_y(\omega)\,d\omega.$$

In the nonlinear case, we replace the feedback gain N with $N_r(\sigma_y)$ so that

$$\tilde{H}_{yd}(s) = \frac{P(s)}{1 + P(s)N_r(\sigma_y)}, \qquad \sigma_y = \frac{1}{2\pi}\int_{-\infty}^{\infty} \tilde{H}_{yd}(-i\omega)S_d(\omega)\tilde{H}_{yd}(i\omega). \tag{3.26}$$

Note that this equation gives an algebraic relationship for σ_y that can be solved and then used to compute $N_r(\sigma)$ and $S_y(\omega)$.

Consider next the case of both a limit cycle and random noise,

$$y(t) = a\sin(\omega t + \phi) + r(t).$$

We now look for solutions of the coupled equations

$$\tilde{H}_{yd}(s) = \frac{P(s)}{1 + P(s)N_r(\sigma_y)}, \qquad \sigma_y = \frac{1}{2\pi}\int_{-\infty}^{\infty} \tilde{H}_{yd}(-i\omega)S_d(\omega)\tilde{H}_{yd}(i\omega),$$

$$N_a(a,\sigma_y)P(i\omega_0) = -1. \tag{3.27}$$

---

[1]These are described in more detail in Chapter 4.

If we can find a, σ_y and ω_0 that satisfy all of the equations, then we get a description of $y(t)$.

It is interesting to note that it can sometimes happen that $S_d(\omega)$ can cause an unstable (noiseless) system to be stable. Similarly, we can get a system with $N_r(0, \sigma_y)$ that destabilizes and otherwise stable system.

3.7   Bifurcations

Hopf bifurcation is a technique that is often used to understand whether a system admits a periodic orbit when some parameter is varied. Usually, such an orbit is a small amplitude periodic orbit that is present in the close vicinity of an unstable steady state.

Consider the system dependent on a parameter α:

$$\dot{x} = g(x, \alpha), x \in \mathbb{R}^n, \ \alpha \in \mathbb{R},$$

and assume that at the steady state $\bar{x}$ corresponding to $\alpha = \bar{\alpha}$ (i.e., $g(\bar{x}, \bar{\alpha}) = 0$), the linearization $\frac{\partial g}{\partial x}(\bar{x}, \bar{\alpha})$ has a pair of (non zero) imaginary eigenvalues with the remaining eigenvalues having negative real parts. Define the new parameter $\mu := \alpha - \bar{\alpha}$ and re-define the system as

$$\dot{x} = f(x, \mu) := g(x, \mu + \bar{\alpha}),$$

so that the linearization $\frac{\partial f}{\partial x}(\bar{x}, 0)$ has a pair of (non zero) imaginary eigenvalues with the remaining eigenvalues having negative real parts. Denote by $\lambda(\mu) = \beta(\mu) + i\omega(\mu)$ the eigenvalue such that $\beta(0) = 0$. Then, if $\frac{\partial \beta}{\partial \mu}(\mu = 0) \neq 0$ the system admits a small amplitude almost sinusoidal periodic orbit for μ small enough and the system is said to go through a Hopf bifurcation at $\mu = 0$. If the small amplitude periodic orbit is stable, the Hopf bifurcation is said *supercritical*, while if it is unstable it is said *subcritical*. Figure 3.20 shows diagrams corresponding to these bifurcations.

In order to determine whether a Hopf bifurcation is supercritical or subcritical, it is necessary to calculate a "curvature" coefficient, for which there are formulas (Marsden and McCrocken, 1976) and available bifurcation software, such as AUTO. In practice, it is often enough to calculate the value $\bar{\alpha}$ of the parameter at which Hopf bifurcation occurs and simulate the system for values of the parameter α close to $\bar{\alpha}$. If a small amplitude limit cycle appears, then the bifurcation must be supercritical.

The Hopf bifurcation result is based on the center manifold theory for nonlinear dynamical systems. For a rigorous treatment of Hopf bifurcation is thus necessary to study center manifold theory first, which is outside the scope of this text. For details, the reader is referred to Wiggins book on dynamical systems and chaos.
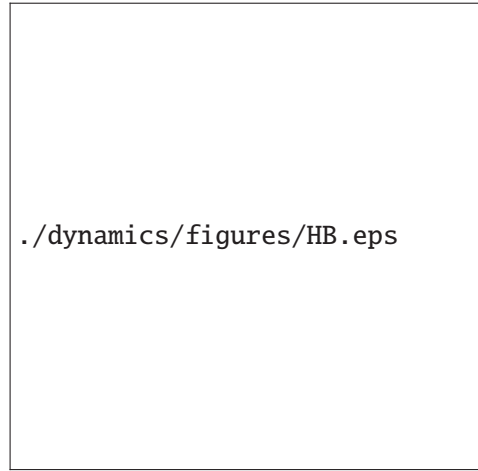
Figure 3.20: Hopf Bifurcation.

3.8 Model Reduction Techniques

The techniques that we have developed in this chapter can be applied to a wide variety of dynamical systems. However, many of the methods require significant computation and hence we would like to reduce the complexity of the models as much as possible before applying them. In this section we review methods for doing such a reduction in the complexity of the models. Most of the techniques are based on the common idea that if we are interested in the slower time scale dynamics of a system, the fast time scale dynamics can be approximated by their equilibrium solutions. This idea was introduced in Chapter 2 in the context of reduced order mechanisms; we present a more mathematical analysis of such systems here.

Singular perturbation analysis

Let $(x, y) \in D := D_x \times D_y \subset \mathbb{R}^n \times \mathbb{R}^m$ and consider the vector field

$$\dot{x} = f(x, y), \quad \epsilon \dot{y} = g(x, y), \quad (x(0), y(0)) = (x_0, y_0)$$

in which $0 < \epsilon \ll 1$ is a small parameter. Since $\epsilon \ll 1$, the absolute value of the time derivative of y can be much larger than the time derivative of x, resulting in y dynamics that are much faster than the x dynamics. That is, this system has a slow time scale evolution (in x) and a fast time-scale evolution (in y). If we are interested only in the slower time scale, then the above system can be approximated (under suitable conditions) by the *reduced system*

$$\dot{\bar{x}} = f(\bar{x}, \bar{y}), \quad 0 = g(\bar{x}, \bar{y}), \quad \bar{x}(0) = x_0.$$

Letting $y = \gamma(x)$ (called the *slow manifold*) be the locally unique solution of $g(x, y) = 0$, we can approximate the dynamics in x as

$$\dot{\bar{x}} = f(\bar{x}, \gamma(\bar{x})), \ x(0) = x_0.$$

We seek to determine under what conditions the solution $x(t)$ is "close" to the solution $\bar{x}(t)$ of the reduced system. This problem can be addressed by analyzing the fast dynamics. Letting $\tau = t/\epsilon$ be the fast time scale, we have that

$$\frac{dx}{d\tau} = \epsilon f(x, y), \qquad \frac{dy}{d\tau} = g(x, y), \qquad (x(0), y(0)) = (x_0, y_0),$$

so that when $\epsilon \ll 1$, $x(\tau)$ does not appreciably change. Therefore, the above system in the τ time scale can be approximated by

$$\frac{dy}{d\tau} = g(x_0, y), \qquad y(0) = y_0,$$

in which x is "frozen" at the initial condition. This system is usually referred to as the *boundary layer* system. If for all x_0, we have that $y(\tau)$ converges to $\gamma(x_0)$, then for $t > 0$ we will have that the solution $x(t)$ is well approximated by the solution $\bar{x}(t)$ to the reduced system. This qualitative explanation is more precisely captured by the following theorem (originally due to Tikonov).

Theorem 3.7. *Assume that*

$$\frac{\partial}{\partial y} g(x, y)\bigg|_{y=\gamma(x)} < 0$$

uniformly for $x \in D_x$. Let the solution of the reduced system be uniquely defined for $t \in [0, t_f]$. Then, for all $t_b \in (0, t_f]$ there is a constant $\epsilon^* > 0$ and set $\Omega \subseteq D$ such that

$$x(t) - \bar{x}(t) = O(\epsilon) \text{ uniformly for } t \in [0, t_f],$$
$$y(t) - \gamma(\bar{x}(t)) = O(\epsilon) \text{ uniformly for } t \in [t_b, t_f],$$

provided $\epsilon < \epsilon^*$ and $(x_0, y_0) \in \Omega$.

Example 3.9 (Linear system)**.** Consider the following linear system

$$\begin{aligned} \dot{x}_1 &= -x_1 \\ \dot{x}_2 &= -\frac{1}{\epsilon} x_2 + \frac{1}{\epsilon} x_1, \ \epsilon > 0, \end{aligned} \qquad (3.28)$$

in which ϵ is very small. This system has two eigenvalues equal to -1 and $-1/\epsilon$ with corresponding eigenvectors $(1 - \epsilon, 1)$ and $(0, 1)$, respectively. The slow manifold, obtained by multiplying both sides of the second equation in system (3.28)
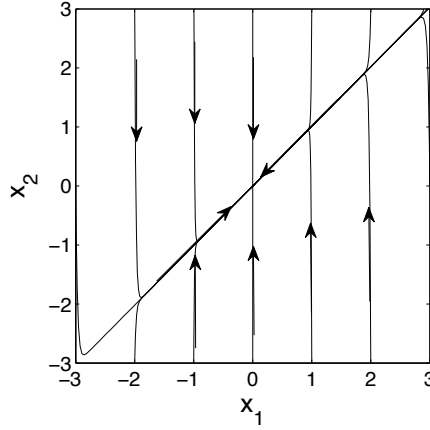
Figure 3.21: Simulation results for the system in equations (3.28). Trajectories in the x_1, x_2 plane.

by ϵ and setting $\epsilon = 0$, is given by $x_2 = x_1$ and the boundary layer system is exponentially stable. The reduced system is just given by

$$\dot{\bar{x}}_1 = -\bar{x}_1, \text{ and } \bar{x}_2(t) = \bar{x}_1(t).$$

The trajectories of the system along with the slow manifold are represented in Figure 3.21. The initial conditions that are not on the slow manifold quickly converge to the slow manifold and then they converge to the origin. ∇

Example 3.10 (Enzymatic reaction). Let's go back to the enzymatic reaction

$$E + S \underset{k_r}{\overset{k_f}{\rightleftharpoons}} C \xrightarrow{k_{cat}} E + P,$$
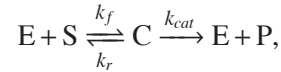
in which E is an enzyme, S is the substrate to which the enzyme binds to form the complex C, and P is the product resulting from the modification of the substrate S due to the binding with the enzyme E. The rate k_f is referred to as association constant, k_r as dissociation constant, and k_{cat} as the catalytic rate. The corresponding ODE system is given by

$$
\begin{aligned}
\frac{dE}{dt} &= -k_f E \cdot S + k_r C + k_{cat} C \\
\frac{dS}{dt} &= -k_f E \cdot S + k_r C \\
\frac{dC}{dt} &= k_f E \cdot S - (k_r + k_{cat}) C \\
\frac{dP}{dt} &= k_{cat} C.
\end{aligned}
$$

By assuming that $k_r, k_f \gg k_{cat}$, we obtained that approximatively $\frac{dC}{dt} = 0$ and thus that $C = \frac{E_{tot}S}{S+K_m}$, with $K_m = \frac{k_r+k_{cat}}{k_f}$ and $\frac{dP}{dt} = \frac{V_{max}S}{S+K_m}$ with $V_{max} = k_{cat}E_{tot}$. From this, it also follows that

$$\frac{dE}{dt} \approx 0 \text{ and } \frac{dS}{dt} \approx -\frac{dP}{dt}. \tag{3.29}$$

How good is this approximation? By applying the singular perturbation method, we will obtain a clear answer to this question. Specifically, define $a := k_f/k_r$ and take the system to standard singular perturbation form by defining the small parameter as $\epsilon := \frac{k_{cat}}{k_r}$, so that $k_f = \frac{k_{cat}}{\epsilon}a$, $k_r = \frac{k_{cat}}{\epsilon}$, and the system becomes

$$\epsilon \frac{dE}{dt} = -ak_{cat}E \cdot S + k_{cat}C + \epsilon k_{cat}C$$

$$\epsilon \frac{dS}{dt} = -ak_{cat}E \cdot S + k_{cat}C$$

$$\epsilon \frac{dC}{dt} = ak_{cat}E \cdot S - k_{cat}C - \epsilon k_{cat}C$$

$$\frac{dP}{dt} = k_{cat}C.$$

One cannot directly apply singular perturbation theory on this system because one can verify from the linearization of the first three equations that the boundary layer dynamics are not locally exponentially stable as there are two zero eigenvalues. This is because the three variables E, S, C are not independent. Specifically, $E = E_{tot} - C$ and $S + C + P = S(0) = S_{tot}$, assuming that initially we have S in amount $S(0)$ and no amount of P and C in the system. Given these conservation laws, the system can be re-written as

$$\epsilon \frac{dC}{dt} = ak_{cat}(E_{tot} - C) \cdot (S_{tot} - C - P) - k_{cat}C - \epsilon k_{cat}C$$

$$\frac{dP}{dt} = k_{cat}C.$$

Under the assumption made in the analysis of the enzymatic reaction that $S_{tot} \gg E_{tot}$, we have that $C \ll S_{tot}$ so that the equations finally become

$$\epsilon \frac{dC}{dt} = ak_{cat}(E_{tot} - C) \cdot (S_{tot} - P) - k_{cat}C - \epsilon k_{cat}C$$

$$\frac{dP}{dt} = k_{cat}C.$$

One can verify (show as an exercise) that in this system, the boundary layer dynamics is locally exponentially stable, so that setting $\epsilon = 0$ one obtains $\bar{C} = \frac{E_{tot}(S_{tot}-\bar{P})}{(S_{tot}-\bar{P})+K_m} =: g(\bar{P})$ and thus that the slow dynamics of the system are given by

$$\frac{d\bar{P}}{dt} = V_{max}\frac{(S_{tot} - \bar{P})}{(S_{tot} - \bar{P}) + K_m}.$$

From the conservation law $\bar{S} + \bar{C} + \bar{P} = S(0) = S_{tot}$, we obtain that $\frac{d\bar{S}}{dt} = -\frac{d\bar{P}}{dt} - \frac{d\bar{C}}{dt}$, in which now $\frac{d\bar{C}}{dt} = \frac{\partial g}{\partial P}(\bar{P}) \cdot \frac{dP}{dt}$. Therefore

$$\frac{d\bar{S}}{dt} = -\frac{d\bar{P}}{dt}\left(1 + \frac{\partial g}{\partial P}(\bar{P})\right), \quad \bar{S}(0) = S_{tot} - g(\bar{P}(0)) - \bar{P}(0) \qquad (3.30)$$

and

$$\frac{d\bar{E}}{dt} = -\frac{d\bar{C}}{dt} = -\frac{\partial g}{\partial P}(\bar{P})\frac{d\bar{P}}{dt}, \quad E(0) = E_{tot} - g(\bar{P}(0)), \qquad (3.31)$$

which are different from expressions (3.29). Specifically, these expressions are close to those in (3.29) only when $\frac{\partial g}{\partial P}(\bar{P})$ is small enough. In the plots of Figure 3.22, we show the time trajectories of the original system, of the Michaelis-Menten quasi-steady state approximation, and of the singular perturbation approximation. The trajectories of $E(t)$ and of $S(t)$ for the quasi-steady state approximation have been obtained from the conservation laws once $P(t)$ and $C(t)$ are determined. The trajectories of these variables for the singular perturbation approximation have been obtained directly integrating equations (3.30) and (3.31). Notice that the quasi-steady state approximations $\frac{dC}{dt} \approx 0$ and $\frac{dE}{dt} \approx 0$ are well representing the dynamics of the C and E variables only while $S(t)$ is large enough. By contrast, equations (3.30-3.31) well represent the system even when the substrate goes to zero. In Figure 3.23, we show the curve $C = g(P)$ (in red) and the trajectories of the full system in black. All of the trajectories of the system immediately collapse into an ϵ-neighbor of the curve $C = g(P)$. $\qquad\qquad\qquad\qquad\qquad\qquad \nabla$

Balanced truncation

Principle component analysis (PCA)

Exercises

3.1 (Frequency response of a phosphorylation cycle) Consider the model of a covalent modification cycle as illustrated in Chapter 2 in which the kinase Z is not constant, but it is produced and decays according to the reaction $Z \underset{u(t)}{\overset{\delta}{\rightleftharpoons}}$. Let $u(t)$ be the input stimulus of the cycle and let X^* be the output. Determine the frequency response of X^* to u, determine its bandwidth, and make plots of it. What parameters can be used to tune the bandwidth?

3.2 (Two gene oscillator) Consider the feedback system composed of two genes expressing proteins A (activator) and R (repressor), in which we denote by A, R, m_A, and m_R, the concentrations of the activator protein, the repressor protein, the mRNA for the activator protein, and the mRNA for the repressor protein, respec-
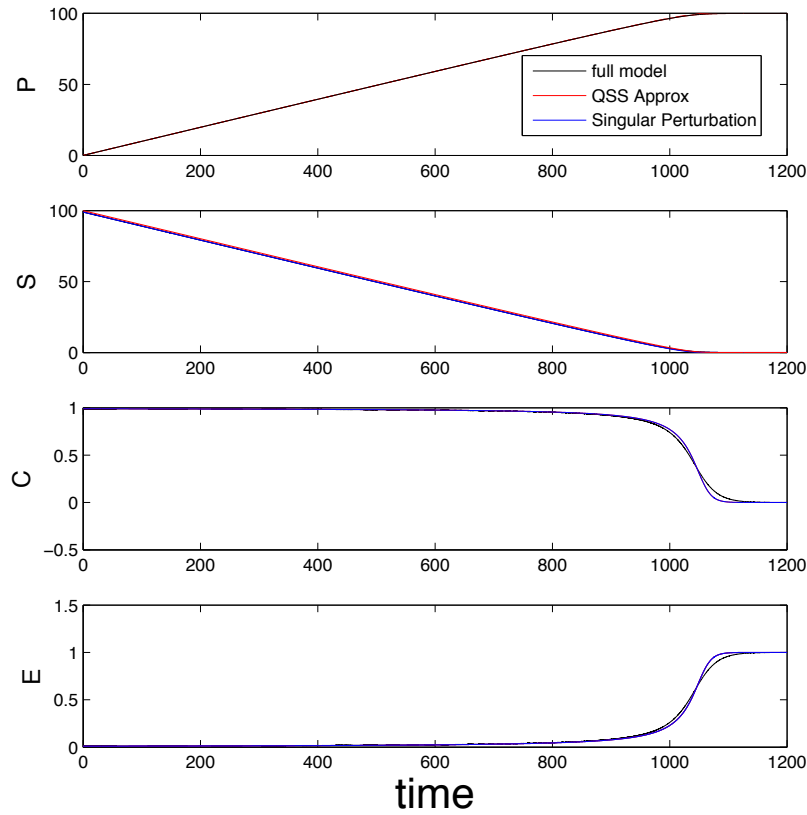
Figure 3.22: Simulation results for the enzymatic reaction comparing the approximations from singular perturbation and from the quasi-steady state approximation. Here, we have $S_{tot} = 100$, $E_{tot} = 1$, $k_r = k_f = 10$, and $k_{cat} = 0.1$.

tively. The ODE model corresponding to this system is given by

$$\frac{dm_A}{dt} = \frac{\alpha_0}{K_1 + R^n} - \gamma m_A \qquad \frac{dm_R}{dt} = \frac{\alpha A^m}{K_2 + A^m} - \gamma m_R$$

$$\frac{dA}{dt} = \beta m_A - \delta A \qquad \frac{dR}{dt} = \beta m_R - \delta R.$$

Determine parameter conditions under which this system admits a stable limit cycle. Validate your finding through simulation.

3.3 (Goodwin oscillator) Consider the simple set of reactions

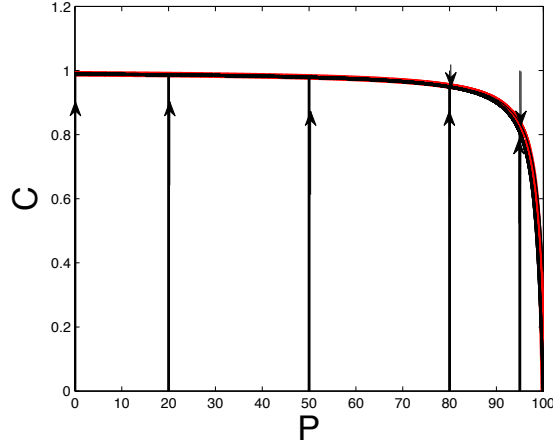$$X_1 \xrightarrow{k} X_2 \xrightarrow{k} X_3 .... \xrightarrow{k} X_n.$$
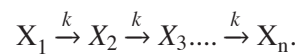
Figure 3.23: The slow manifold of the system $C = g(P)$ is shown in red. In black, we show the trajectories of the the full system. These trajectories collapse into an ϵ-neighbor of the slow manifold. Here, we have $S_{tot} = 100$, $E_{tot} = 1$, $k_r = k_f = 10$, and $k_{cat} = 0.1$.

Assume further that X_n is a transcription factor that represses the production of protein X_1 through transcriptional regulation (assume simple binding of X_1 to DNA). Neglecting the mRNA dynamics of X_1, write down the ODE model of this system and determine conditions on the length n of the cascade for which the system admits a stable limit cycle. Validate your finding through simulation.

3.4 (Activator-repressor clock) A well known oscillating motif is given by the activator-repressor clock by Atkinson et al. [**?**] in which an activator protein A activates its own production and the one of a repressor protein R, which in turn acts as a repressor for A. The ODE model corresponding to this clock is given by

$$\frac{dm_A}{dt} = \frac{\alpha A^m + \alpha_0}{K_1 + R^n + A^m} - \gamma m_A \qquad \frac{dm_R}{dt} = \frac{\alpha A^m}{K_2 + A^m} - \gamma m_R$$

$$\frac{dA}{dt} = \mu(\beta m_A - \delta A) \qquad\qquad \frac{dR}{dt} = \beta m_R - \delta R,$$

in which $\mu > 0$ models the difference of speeds between the dynamics of the activator and that of the repressor. Indeed a key requirement for this system to oscillate is that the dynamics of the activator are sufficiently faster than that of the repressor. Demonstrate that this system goes through a Hopf Bifurcation with bifurcation parameter μ. Validate your findings with simulation by showing the small amplitude periodic orbit.

3.5 (Model reduction via singular perturbation) Consider again the model of a co-valent modification cycle as illustrated in Chapter 2 in which the kinase Z is not constant, but it is produced and decays according to the reaction $Z \underset{u(t)}{\overset{\delta}{\rightleftharpoons}} \emptyset$. Consider

that $k_f, k_r \gg k_{cat}, \delta, u(t)$ and employ singular perturbation with small parameter, for example, $\epsilon = \delta/k_r$ to obtain the approximated dynamics of $Z(t)$ and $X^*(t)$. How is this different from the result obtained in Exercise 2.6? Explain.